Organic solar cells: An overview

Harald Hoppe[a] and Niyazi Serdar Sariciftci
Linz Institute for Organic Solar Cells (LIOS), Physical Chemistry, Johannes Kepler University, 4040 Linz, Austria

(Received 8 March 2004; accepted 12 March 2004)

Organic solar cell research has developed during the past 30 years, but especially in the last decade it has attracted scientific and economic interest triggered by a rapid increase in power conversion efficiencies. This was achieved by the introduction of new materials, improved materials engineering, and more sophisticated device structures. Today, solar power conversion efficiencies in excess of 3% have been accomplished with several device concepts. Though efficiencies of these thin-film organic devices have not yet reached those of their inorganic counterparts ($\eta \approx 10$–20%); the perspective of cheap production (employing, e.g., roll-to-roll processes) drives the development of organic photovoltaic devices further in a dynamic way. The two competitive production techniques used today are either wet solution processing or dry thermal evaporation of the organic constituents. The field of organic solar cells profited well from the development of light-emitting diodes based on similar technologies, which have entered the market recently. We review here the current status of the field of organic solar cells and discuss different production technologies as well as study the important parameters to improve their performance.

I. INTRODUCTION

Though common materials used for photovoltaics (i.e., the conversion of sunlight into electrical energy) are inorganic,[1] there has been a tremendous effort to develop organic solar cells within the last three decades.[2–9] The field started by the application of small organic molecules (pigments),[2,3,9] and since the development of semiconducting polymers,[10–13] these materials were incorporated into organic solar cells resulting in remarkable improvements within the past years.[4,5,8,14] The potential of semiconducting organic materials to transport electric current and to absorb light in the ultraviolet (UV)-visible part of the solar spectrum is due to the sp^2-hybridization of carbon atoms. For example, in conducting polymers the electron in the p_Z-orbital of each sp^2-hybridized carbon atom will form π-bonds with neighboring p_Z electrons in a linear chain of sp^2-hybridized carbon atoms, which leads then to dimerization (an alternating single and double bond structure, i.e., Peierls distortion). Due to the isomeric effect, these π-electrons are of a delocalized nature, resulting in high electronic polarizability.

An important difference to inorganic solid-state semiconductors lies in the generally poor (orders of magnitudes lower) charge-carrier mobility in these materials,[15] which has a large effect on the design and efficiency of organic semiconductor devices. However, organic semiconductors have relatively strong absorption coefficients (usually $\geqslant 10^5$ cm^{-1}), which partly balances low mobilities, giving high absorption in even <100 nm thin devices. Another important difference to crystalline, inorganic semiconductors is the relatively small diffusion length of primary photoexcitations (called excitons) in these rather amorphous and disordered organic materials.[9,16–23] These excitons are an important intermediate in the solar energy conversion process, and usually strong electric fields are required to dissociate them into free charge carriers, which are the desired final products for photovoltaic conversion. This is a consequence of exciton binding energies usually exceeding those of inorganic semiconductors.[24,25] These features of organic semiconducting materials lead generally to devices with very small layer thicknesses of the order $\leqslant$100 nm.

Most of the organic semiconductors are hole conductors and have an optical band gap around 2 eV, which is considerably higher than that of silicon and thus limits the harvesting of the solar spectrum to a great extent. Nevertheless, the chemical flexibility for modifications on organic semiconductors via chemical synthesis methods as well as the perspective of low cost, large-scale production drives the research in this field in academia and industry.

[a]Address all correspondence to this author.
e-mail: harald.hoppe@jku.at
DOI: 10.1557/JMR.2004.0252

The first generation of organic photovoltaic solar cells was based on single organic layers sandwiched between two metal electrodes of different work functions.[2,3] The rectifying behavior of single layer devices was attributed to the asymmetry in the electron and hole injection into the molecular π^* and π-orbitals, respectively,[26] and to the formation of a Schottky-barrier[3,27–29] between the *p*-type (hole conducting) organic layer and the metal with the lower work function. The power conversion efficiencies reported were generally poor (in the range of 10^{-3} to 10^{-2}%), but reached remarkable 0.7% for merocyanine dyes in the early days.[30,31] In this case, the organic layer was sandwiched between a metal–metal oxide and a metal electrode, thus enhancing the Schottky-barrier effect [metal-insulator-semiconductor (MIS)[32] devices]. The next breakthrough was achieved by introducing the bilayer heterojunction concept, in which two organic layers with specific electron or hole transporting properties were sandwiched between the electrodes. Tang reported 1986 about 1% power conversion efficiency for two organic materials (a phtalocyanine derivative as *p*-type semiconductor and a perylene derivative as *n*-type semiconductor) sandwiched between a transparent conducting oxide and a semitransparent metal electrode.[33] This result was for many years the outstanding benchmark and was surmounted only at the turn of the millennium.[34,35] Hiramoto and co-workers did pioneering work introducing the concept of an organic tandem cell structure by stacking two heterojunction devices.[36] They also developed a three layer *p-i-n* like structure with a co-deposited interlayer between the *p*-type (hole conducting) and *n*-type (electron conducting) layers.[37,38] In the meantime, the field of conjugated polymers grew mature, and the first single layer devices based on these newly developed materials were presented.[29,39–41] But also, these polymer single layer devices were showing only power conversion efficiencies of less than 0.1%. The observation of a photoinduced electron transfer from optically excited conjugated polymers to the C_{60} molecule[42,43] and the observation of highly increased photoconductivities upon C_{60} addition to the conjugated polymers[44–46] led to the development of polymer–fullerene bilayer heterojunction[16,47,48] and bulk heterojunction[49,50] devices incorporating C_{60} and C_{60}-derivatives with enhanced solubility.[51] The photoinduced electron transfer occurs when it is energetically favorable for the electron in the S_1-excited state of the polymer to be transferred to the much more electronegative C_{60}, thus resulting in an effective quenching of the excitonic photoluminescence of the polymer.[42] Because the electron is transferred from a *p*-type hole conducting polymer onto the rather *n*-type electron conducting C_{60} molecule, the notation of donor (D) and acceptor (A) with respect to the electron transfer was introduced. The photoinduced charge transfer is depicted schematically in Fig. 1 together with the energetic description.

The bulk heterojunction concept, similar to the co-evaporated molecular structures of Hiramoto,[37,38] was introduced by blending two polymers having donor (D) and acceptor (A) properties in solution.[52–54] Spin cast films from such binary solutions then resulted in solid-state mixtures of both polymers. A further approach was lamination of two polymer layers, leading to a diffusive interface between D and A moieties, and calculated power conversion efficiencies approaching 2% were reported.[55]

The organic solar cell development gained momentum in the past years: Conversion efficiencies between 1.5 and 4% have been achieved for evaporated bilayer devices,[56–58] bulk heterojunction polymer–fullerene

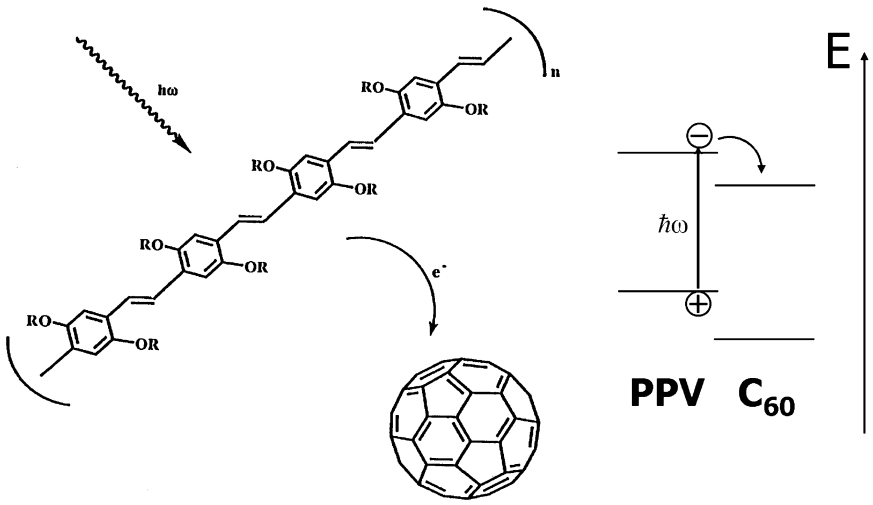

FIG. 1. Illustration of the photoinduced charge transfer (left) with a sketch of the energy level scheme (right). After excitation in the PPV polymer, the electron is transferred to the C_{60} due to its higher electron affinity.

devices,[59–66] co-evaporated molecular devices,[67–70] and in organic–inorganic hybrid devices.[71–73]

Conceptually similar to the bulk heterjunction, there is a wide research field of dye sensitized, electrochemical solar cells. The early steps in the development[74–79] were largely improved by the Graetzel group.[80] To review this field of electrochemical photovoltaic cells would be beyond the scope of this article, and the interested reader is advised to read the literature in this research area (e.g., Refs. 82–84). However, in recent years, by the introduction of organic hole conductors[19,71,72,84–89] as replacement for the liquid electrolytes in electrochemical solar cells and by the exchange of the electron conducting acceptor materials in organic heterojunction devices with inorganic nanocrystals,[73,90–95] electrochemical and organic photovoltaic research directions are gradually merging together.

For practical application, not only the power conversion efficiency but also the lifetime of the photovoltaic device is of importance. The stability of organic solar cells is mainly affected by photodegradation of the active materials.[60,96,97] However, encapsulation techniques as applied in organic light-emitting diodes (LEDs) can provide an efficient sealing against oxidizing agents, but still a high intrinsic photostability of the organic materials is required.

In the next section, we briefly introduce commonly used materials, followed by a section discussing the main preparation techniques for organic solar cell devices. Thereafter, basic operation principles of photovoltaic light conversion are reviewed, followed by a section presenting the different types of devices. Finally, a section on the control of performance-limiting factors will review recent developments, and promising new approaches are discussed as outlook.

II. MATERIALS

Plants use the natural process of photosynthesis to convert sunlight into chemical energy, where the first step in this process is the absorption of light by the chlorophyll molecule. Interestingly, chlorophyll pigments were also directly applied in a single layer solar cell.[98] Besides the absorption of sunlight and (subsequent) creation of photogenerated charge carriers, a second requirement for solar cell materials is the ability to transport these charge carriers. Both properties are commonly found for materials that have an extended delocalized π-electron system. Phthalocyanine is a representative of the *p*-type, hole-conducting materials that work as electron donor. The perylene and its derivatives show an *n*-type, electron-conducting behavior, and they serve as electron acceptor material. Both of these molecules were often incorporated into evaporated solar cells. Because the optical band-gap of most organic materials is around 2 eV, the thermally excited, intrinsic charge carrier concentrations are rather low. Due to disorder and limited overlap of electronic wavefunctions (van der Waals interactions), also the charge carrier mobilities of organic materials are relatively small and hence they can nearly be regarded as insulators. However, there are possibilities to increase the charge carrier concentration, mostly done via molecular or electrochemical doping. Donor type materials show a doping effect when exposed to oxygen or other strong oxidizing agents such as iodine.[2,3,99] This doping is achieved by transferring an electron from the ground state S_0 of the organic semiconductor to the oxidizing agent, resulting in increased charge carrier concentrations in the hole conductor. As an example for *n*-type doping, perylene was doped upon exposition to hydrogen.[99] Due to these doping effects, the formerly rather insulating materials posses free charge carriers and bilayer devices can work like classical *p-n* junctions.[100,101] However, doping with gases is not very well controllable. A more controlled approach of doping is achieved by the co-evaporation of both materials, matrix and dopant.[69,102–104] Among others, the buckminster fullerene C_{60} (and derivatives) is a strong electron acceptor.[105] Blended with hole-conducting materials, it does not improve charge transport in the dark, but leads to a large increase in photoconductivity under illumination.[44–46] This is a result of the photoinduced charge transfer,[42] and hence this process can be viewed as "photodoping".[106] The chemical structures of some molecular materials are depicted in Fig. 2 [ZnPc (zinc-phthalocyanine), MePtcdi (N,N′-dimethyl-perylene-3,4,9,10-dicarboximide), and C_{60}]. In Fig. 3, some commonly used conjugated polymers are shown. Three important representatives of hole-conducting donor type polymers are MDMO-PPV (poly[2-methoxy-5-(3,7-dimethyloctyloxy)]-1,4-phenylenevinylene), P3HT (poly(3-hexylthiophene-2,5-diyl) and PFB (poly(9,9'-dioctylfluorene-co-bis-*N,N*'-(4-butylphenyl)-bis-*N,N*'-phenyl-1,4-phenylenediamine). They are shown together with electron-conducting acceptor polymers like CN-MEH-PPV (poly-[2-methoxy-5-(2'-ethylhexyloxy)-1,4-(1-cyanovinylene)-phenylene) and F8TB (poly(9,9'-dioctylfluoreneco-benzothiadiazole) and a soluble derivative of C_{60}, namely PCBM (1-(3-methoxycarbonyl) propyl-1-phenyl[6,6]C_{61}). All of these materials are solution processible due to their side-chain solubilization, and the polymers show photo- and electroluminescence.[107–109] For the construction of donor–acceptor solar cells, the donor polymers can be either combined with an acceptor polymer or with fullerenes either in planar or diffuse bilayer structures or in blends (compare Sec. IV). To display the fraction of the sunlight, which can contribute to energy conversion in these materials, absorption coefficients of films of some materials are shown in

https://doi.org/10.1557/JMR.2004.0252

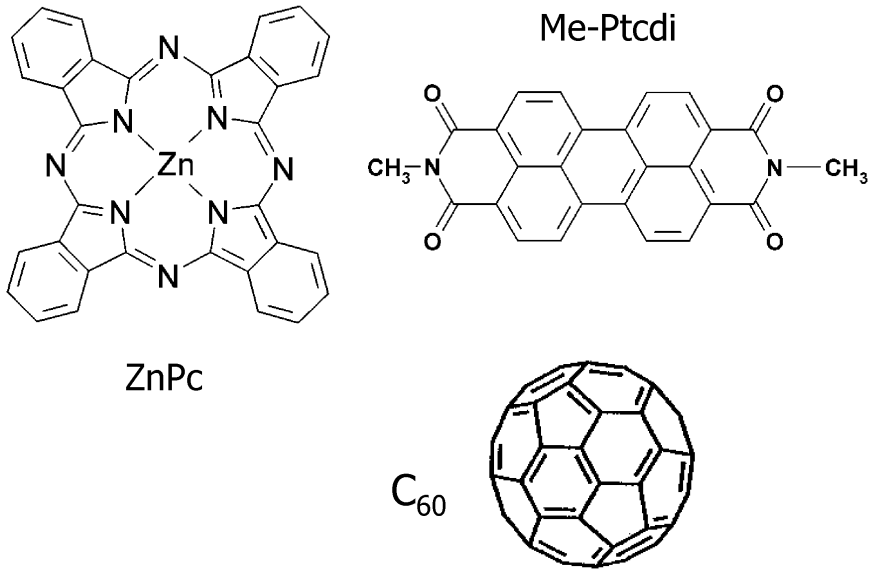

FIG. 2. Some organic molecules commonly applied in evaporated organic solar cells: ZnPc (zinc-phthalocyanine), Me-Ptcdi (N,N'-dimethyl-perylene-3,4,9,10-dicarboximide), and the buckminster fullerene C_{60}.

comparison with the air mass (AM) 1.5 standard solar spectrum in Fig. 4. Though the silicon absorption spectrum extends up to 1100 nm, the organic materials use only the blue side of the solar spectrum.

Charge carrier mobilities in films of molecules and conjugated polymers often depend on the nanoscopic order, which can be manipulated by the preparation conditions.[110–113] For example, a preferential orientation of polymer backbones parallel to the substrate[114,115] gives rise to an anisotropic charge transport.[112,113] An overview on some materials used for organic field-effect transistors (FETs) is reported by Dimitrakopoulos.[15] However, charge transport in FETs is in lateral direction (parallel to the substrate) contrary to solar cells and most LEDs. For bulk heterojunction solar cells, it was observed that the charge transport in such blend structures is a sensitive function of the nanomorphology of the mixture.[116–119]

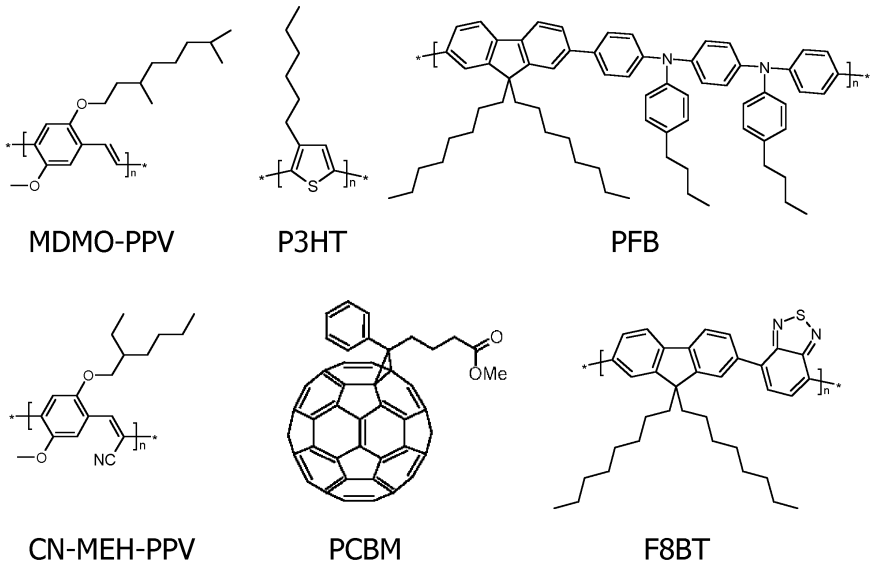

FIG. 3. Several solution processible conjugated polymers and a fullerene derivative used in organic solar cells. Upper row: the *p*-type hole-conducting donor polymers MDMO-PPV (poly[2-methoxy-5-(3,7-dimethyloctyloxy)]-1,4-phenylenevinylene), P3HT (poly(3-hexylthiophene-2,5-diyl) and PFB (poly(9,9'-dioctylfluorene-co-bis-*N,N*'-(4-butylphenyl)-bis-*N,N*'-phenyl-1,4-phenylenediamine). Lower row: the electron-conducting acceptor polymers CN-MEH-PPV (poly-[2-methoxy-5-(2'-ethylhexyloxy)-1,4-(1-cyanovinylene)-phenylene) and F8TB (poly(9,9'-dioctylfluoreneco-benzothiadiazole) and a soluble derivative of C_{60}, PCBM (1-(3-methoxycarbonyl) propyl-1-phenyl[6,6]C_{61}).

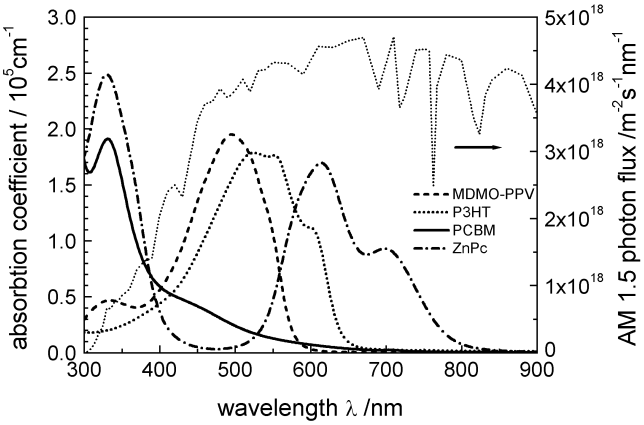

FIG. 4. Absorption coefficients of films of commonly used materials are depicted in comparison with the standard AM 1.5 terrestrial solar spectrum. The overlap is generally small.

III. PREPARATION TECHNIQUES

The two most common techniques for thin film production are in a way complementary for the choice of materials. Whereas for evaporation thermal stability is required, materials for solution processing need to be soluble. Small molecules may be thermally more stable but less soluble than polymers, where solubility often is achieved by side-chain solubilization. Polymers will decompose under excessive heat and have a too large molar mass for evaporation. Hence for small molecules, evaporation is the best choice, whereas semiconducting polymers are mainly processed from solution. However, less soluble molecules like C_{60} may become soluble when modified by attaching solubilizing groups (e.g., PCBM) and short polymers or oligomers may also be evaporated.[67,120]

A. Evaporation

To grow films by thermal evaporation, usually a vacuum of $<10^{-5}$ mbar is applied. Thus the mean free path of the evaporated molecule is longer than the distance between the evaporation source and the sample holder. In addition, contaminants like oxygen and water are reduced and can be eliminated further by ultra high vacuum ($<10^{-9}$ mbar) or evaporation inside of a glove box with inert atmosphere. To create interpenetrating donor-acceptor networks or to achieve molecular doping, co-evaporation techniques can be applied.[37,67,69,102,121]

B. Wet processing

Common to all wet processing techniques is the solving of organic materials in an appropriate solvent like water or any other polar or nonpolar organic solvent. A special case is the solution processing of a soluble monomer coupled with a polymerization reaction during (e.g., electrochemical polymerization) or after (e.g., via heat treatment, UV curing, and so forth) the film forming process (precursor route). This has the advantage that after preparation, the resulting polymers are insoluble and another film can be deposited from solution on top of them. If polymers or polymer/polymer or polymer/molecule blends are directly processed from solution, several common techniques are applied: (i) spin coating, (ii) doctor blading, (iii) screen-printing, (iv) inkjet printing, and many more. For example, screen-printing was applied to a MDMO-PPV:PCBM blend (Fig. 5).[122] This exploitation of existing printing techniques assures an easy upscaling of the production and low energy consumption during production of solar cells, which is important for the energy amortization (energy delivered by a solar cell during its lifetime as compared to the energy needed to produce the solar cell itself).

IV. BASIC WORKING PRINCIPLES

The process of converting light into electric current in an organic photovoltaic cell is accomplished by four consecutive steps: (i) *Absorption* of a photon leading to the formation of an excited state, the electron-hole pair (exciton). (ii) *Exciton diffusion* to a region, where (iii) the *charge separation* occurs. (iv) Finally the *charge transport* to the anode (holes) and cathode (electrons), to supply a direct current for the consumer load.

The potential energy stored within one pair of separated positive and negative charges is equivalent to the difference in their respective quasi-Fermi levels, or in other words it corresponds to the difference in the electrochemical potentials.[25] The larger the quasi-Fermi level splitting remains during charge transport through the interfaces at the contacts, the larger will be the photovoltage. Though for ideal (ohmic) contacts no loss is expected, energy level offsets or band bending at non-ideal contacts (that undergo energy-level-alignments due to Fermi-level differences) can lead to a decrease in the photovoltage.

The electric current that a photovoltaic solar cell delivers corresponds to the number of created charges that are collected at the electrodes. This number depends on the fraction of photons absorbed (η_{abs}), the fraction of electron-hole pairs that are dissociated (η_{diss}), and finally

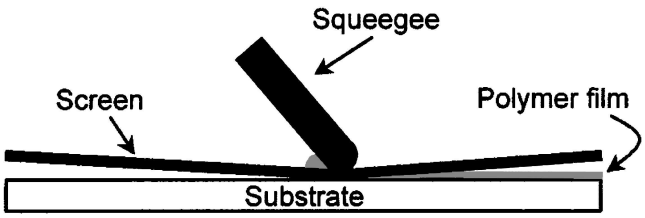

FIG. 5. Schematic of the screen-printing of a polymer/fullerene–based organic solar cell. (Reprinted with permission from Ref. 122. Copyright 2001, American Institute of Physics.)

https://doi.org/10.1557/JMR.2004.0252

the fraction of (separated) charges that reach the electrodes (η_{out}) determining the overall photocurrent efficiency (η_j)

$$\eta_j = \eta_{abs} \times \eta_{diss} \times \eta_{out} \quad .$$

The fraction of absorbed photons is a function of the absorption spectrum, the absorption coefficient, the absorbing layer thickness, and of internal multiple reflections at, for example, metallic electrodes. The fraction of dissociated electron-hole pairs on the other hand is determined by whether they diffuse into a region where charge separation occurs and on the charge separation probability there.[123]

To reach the electrodes, the charge carriers need a net driving force, which generally results from a gradient in the electrochemical potentials of electrons and holes. Two "forces" contribute to this: internal electric fields and concentration gradients of the respective charge carrier species. The first leads to a field induced drift and the other to a diffusion current. Though a detailed analysis requires the knowledge of charge carrier distributions over film depth, thin film devices (<100 nm) are mostly field drift dominated, whereas thick devices, having effective screening of the electrical fields inside the bulk, are more dominated by the diffusion of charge carriers in concentration gradients at the selective contacts.

To understand the rectifying behavior of an intrinsic (nondoped) semiconductor device in the dark, the MIM (metal-insulator-metal) model[32] is useful. In Fig. 6, a semiconductor, sandwiched between two metal electrodes with different work functions is depicted for several situations. The metals are represented by their Fermi levels, whereas for the semiconductor the valence and conduction bands, corresponding to the molecular LUMO (lowest unoccupied molecular orbital) and the HOMO (highest occupied molecular orbital) levels, are shown. In Fig. 6(a), there is no voltage applied (i.e., short-circuit conditions). Hence, there is no net current flowing in the dark, and the built-in electric field resulting from the difference in the metals' work functions is evenly distributed throughout the device. Under illumination, separated charge carriers can drift in this electric field to the respective contacts: the electrons move to the lower work function metal and the holes to the opposite. The device then works as a solar cell. In Fig 6(b), the situation is shown for open circuit conditions, also known as "flat band condition." The applied voltage is called the open circuit voltage V_{OC}, which corresponds in this case to the difference in the metals' work functions and balances the built-in field. As there is no net driving force for the charge carriers, the current is zero. In Fig. 6(c) the situation is shown for an applied reverse bias and only a very small injected dark current j_0 can flow. Under illumination, the generated charge carriers drift under strong electric fields to the respective electrodes and the diode works as a photodetector. If a forward bias larger than the open circuit voltage is applied [Fig. 6(d)], the contacts can efficiently inject charges into the semiconductor. If these can recombine radiatively,

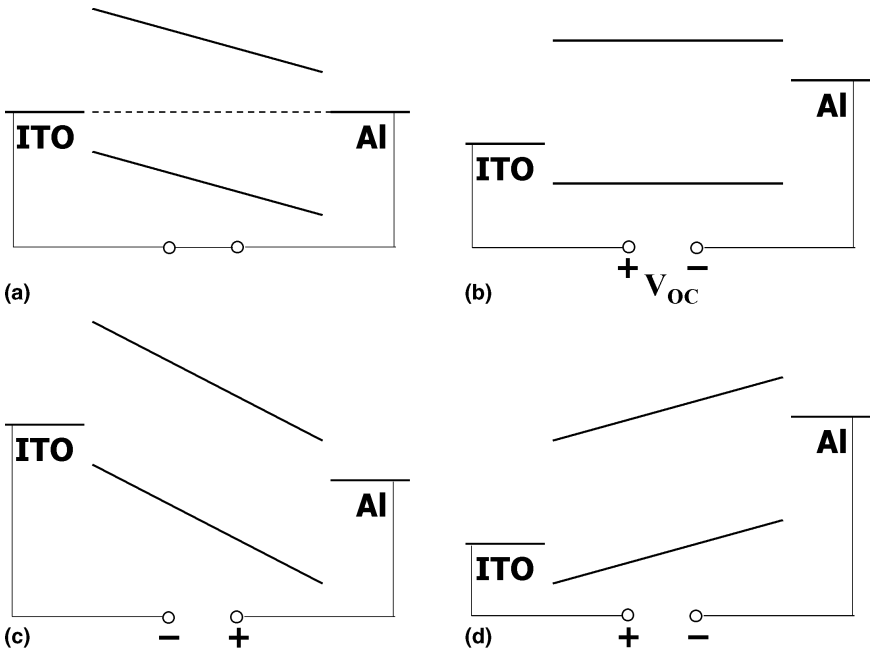

FIG. 6. Metal-insulator-metal (MIM) picture of organic diode device function. (a) Closed circuit condition: under illumination photogenerated charges drift toward the contacts. (b) Flat band or open circuit condition: the current becomes zero. (c) Reversed bias: photogenerated charges drift in strong electric fields, the diode operates as a photodetector. (d) Forward bias larger than V_{OC}: the injection increases and the diode opens up.

https://doi.org/10.1557/JMR.2004.0252

the device works as a LED. The asymmetric diode behavior results basically from the different injection of the two metals into the HOMO and LUMO levels, respectively, which depends exponentially on the energy barrier between them.[26]

In Fig. 7, the current-voltage characteristics are shown for a solar cell in the dark and under illumination. In the dark, there is almost no current flowing, until the contacts start to inject heavily at forward bias for voltages larger than the open circuit voltage. Under illumination, the current flows in the opposite direction than the injected currents. At (a) the maximum generated photocurrent flows under short-circuit conditions; at (b) the photogenerated current is balanced to zero (flat band condition). Between (a) and (b), in the fourth quadrant, the device generates power (i.e., current × voltage). At a certain point, denoted as maximum power point (MPP), the product between current and voltage and hence the power output is largest. To determine the efficiency of a solar cell, this power needs to be compared with the incident light intensity. Generally, the filling factor (FF) is calculated as $FF = V_{MPP} \times I_{MPP}/(V_{OC} \times I_{SC})$ to denote the part of the product of V_{OC} and I_{SC} that can be used. With this, the power conversion efficiency can be written as

$$\eta_{POWER} = \frac{P_{OUT}}{P_{IN}} = \frac{I_{MPP} \cdot V_{MPP}}{P_{IN}} = \frac{FF \cdot I_{SC} \cdot V_{OC}}{P_{IN}} \quad . \tag{1}$$

Generally, the I-V characteristics of a photovoltaic device can be described by

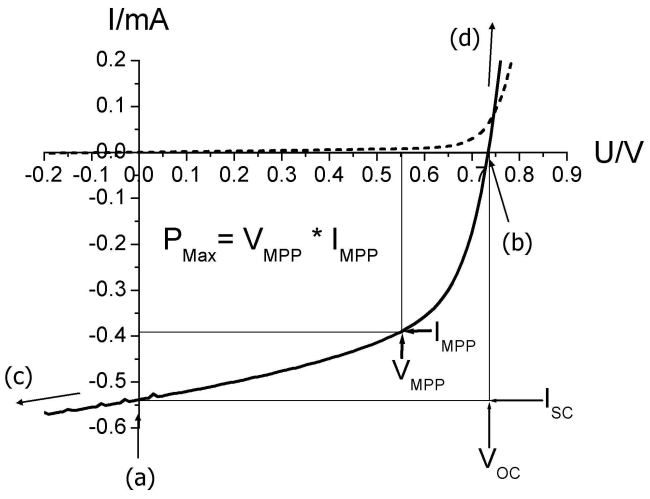

FIG. 7. Current-voltage (IV) curves of an organic solar cell (dark, dashed; illuminated, full line). The characteristic intersections with the abscissa and the ordinate are the open circuit voltage (V_{OC}) and the short-circuit current (I_{SC}), respectively. The largest power output (P_{Max}) is determined by the point where the product of voltage and current is maximized. Division of P_{Max} by the product of I_{SC} and V_{OC} yields the filling factor FF. The letters (a–d) correspond to Fig. 6.

$$I = I_0 \cdot \left\{ \exp\left(\frac{e}{nkT} (U - IR_S) \right) - 1 \right\} + \frac{U - IR_S}{R_{SH}} - I_{PH} \quad , \tag{2}$$

where I_0 is the dark current, e the elementary charge, n the diode ideality factor, U the applied voltage, R_S the series, R_{SH} the shunt resistance, and I_{PH} is the photocurrent. The corresponding equivalent circuit is depicted in Fig. 8. For a high FF, two things are required: (i) that the shunt resistance is very large to prevent leakage currents and (ii) that the series resistance is very low to get a sharp rise in the forward current. The series resistance simply adds up from all series resistance contributions in the device, that is, from bulk transport, from interface transfer and from transport through the contacts.

V. DEVICE ARCHITECTURES

As the exciton binding energy in organic semiconductors is generally large (0.1–1eV) compared to silicon,[24,25,124] the built-in electric fields (on the order of 10^6–10^7 V/m) are usually not high enough to dissociate the excitons directly. Hence, a process has to be introduced that efficiently separates the bound electron-hole pairs. This is possible at the sharp drop of potential at donor–acceptor (D-A) as well as semiconductor–metal interfaces. In the following, the most basic device architectures are reviewed, and the individual advantages and disadvantages are discussed. Their main difference lies in the exciton dissociation or charge separation process, which occurs at different locations within the photoactive layer. A second issue is the consecutive charge transport to the electrodes.

A. Single layer

The first organic solar cells were based on single thermally evaporated molecular organic layers sandwiched between two metal electrodes of different work functions. The rectifying behavior of these devices can be explained by the MIM-model (for insulators) or by the formation of a Schottky barrier (for doped materials) between the metal with the lower work function and the

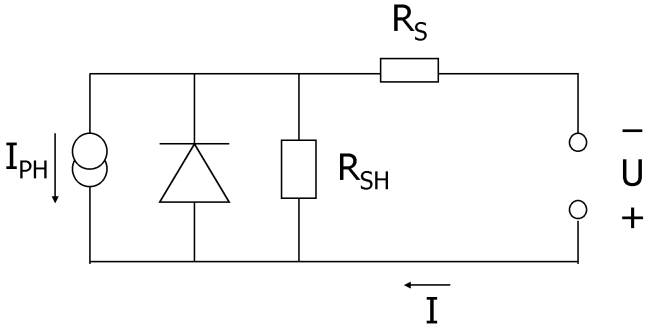

FIG. 8. Equivalent circuit for a solar cell, described by Eq. (2).

https://doi.org/10.1557/JMR.2004.0252

p-type organic layer.[32] In Fig. 9, the situation is depicted for the case of a Schottky junction at the aluminum contact. Close to the contact, in the depletion region W, a resulting band bending from the Schottky contact is depicted. This corresponds to an electric field in which excitons can be dissociated. Therefore, illumination from the two different semitransparent metal contacts can lead to symbatic (proportional to the absorption coefficient) and antibatic behavior of the spectral photocurrent.[3,28,98] Because the exciton diffusion length for most organic solar cell materials is below 20 nm, only those excitons generated in a small region within ≤20 nm from the contacts contribute to the photocurrent. Due to the high series resistances, these materials show a low FF and a field-dependent charge carrier collection. These thin film devices can work well as photodetectors, as under a high reverse bias the electric field drives the created charges to the electrodes. The illumination intensity dependence of the short-circuit photocurrent was sublinear, as expected for bimolecular recombination, as the probability for recombination is proportional to both electron and hole concentrations.

B. Bilayer heterojunction

In a bilayer device, a donor and an acceptor material are stacked together with a planar interface. There the charge separation occurs,[9,21,33,101] which is mediated by a large potential drop between donor and acceptor. The bilayer is sandwiched between two electrodes matching the donor HOMO and the acceptor LUMO, for efficient extraction of the corresponding charge carriers. The bilayer device structure is schematically depicted in Fig. 10, neglecting all kinds of possible band bending due to energy level alignments. Though the formation of a classical *p/n*-junction requires doped semiconductors with free charge carriers to form the electric field in the depleted region, the charge transfer in bilayer heterojunction between undoped donor and acceptor materials is due to the differences in the ionization potential and electron affinity of the adjacent materials (compare Fig. 1). Upon photon absorption in the donor D, the electron is excited from the HOMO to the LUMO ($S^0 \rightarrow S^1$). If now an acceptor molecule A is in close proximity, the electron may be transferred to the LUMO of A, which is energetically preferential when

$$I_{D^*} - A_A - U_C < 0 \quad ,$$

where I_{D^*} is the ionization potential of the excited state (D*) of the donor, A_A the electron affinity of the acceptor, and U_C the effective Coulomb interaction, respectively.[42]

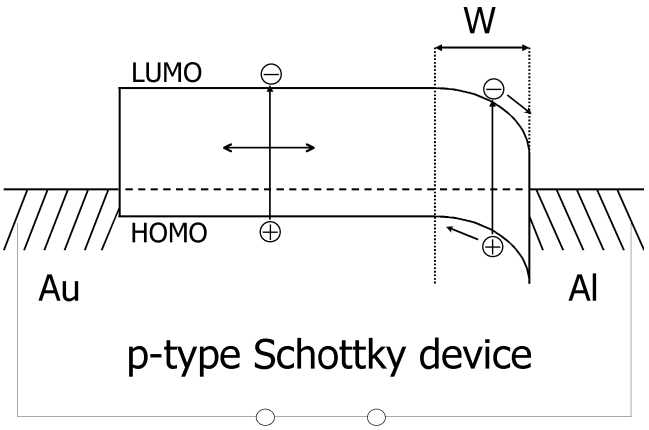

FIG. 9. Schematic of a single layer device with a Schottky contact at the aluminum contact. Photogenerated excitons can only be dissociated in a thin depletion layer W, and thus the device is exciton diffusion limited.

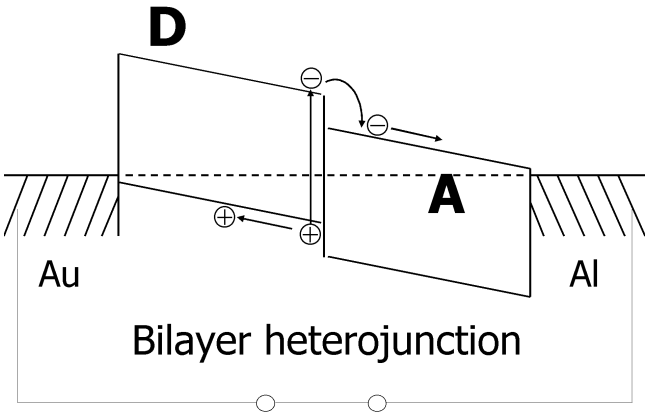

FIG. 10. Schematic of a bilayer heterojunction device. The donor (D) contacts the higher and the acceptor (A) the lower work function metal, to achieve good hole and electron collection, respectively. Photogenerated excitons can only be dissociated in a thin layer at the heterojunction and thus the device is exciton diffusion limited.

The release in electron energy may then be used to separate electron and hole from their Coulomb potential. It is noteworthy that this photoinduced charge transfer (CT) only occurs under illumination, as it needs the excitation energy of the electron in the donor to reach the LUMO in the acceptor. There are experimental indications[125–127] supported by theoretical considerations[128] for the formation of an interfacial dipole between the donor and acceptor phases, independent of illumination. This can stabilize the charge-separated state by a repulsive interaction between the interface and the free charges.[128] Therefore, the success of the D-A concept lays to a great extent in the relative stability of the charge separated state: the recombination rate between holes in D and electrons in A is several orders of magnitude smaller than the forward charge transfer rate.[106,129,130]

A big advantage over the single layer device is the monomolecular charge transport. After the excitons are dissociated at the materials interface, the electrons travel within the *n*-type acceptor, and the holes travel within the *p*-type donor material. Hence, holes and electrons are

effectively separated from each other, and thus charge recombination is greatly reduced and depends more on trap densities. As a consequence, the photocurrent dependency on illumination intensity can be linear,[9,21,28,47,101] and for thinner layers, larger filling factors can be achieved.[33]

Bilayer devices can be produced either by sequential thermal deposition of pigments,[9,28,33,99,101] by solution casting of one soluble material and evaporation of a second layer,[16,17,47,48,131] or by sequential solution casting applying a polymer precursor route.[132] Power conversion efficiencies of about 3.6% under Sun AM 1.5 solar illumination with this geometry were reported with an evaporated bilayer device using copper phthalocyanine and C_{60}.[56–58]

C. Bulk heterojunction

The essence of the bulk heterojunction is to intimately mix the donor and acceptor components in a bulk volume so that each donor–acceptor interface is within a distance less than the exciton diffusion length of each absorbing site. In Fig. 11, the situation is schematically shown for a bulk heterojunction device, again neglecting all kinds of energy level alignments and interface effects. The bulk heterojunction device is similar to the bilayer device with respect to the D-A concept, but it exhibits a largely increased interfacial area where charge separation occurs. Due to the interface being dispersed throughout the bulk, no loss due to too small exciton diffusion lengths is expected, because ideally all excitons will be dissociated within their lifetime. In this conception the charges are also separated within the different phases, and hence recombination is reduced to a large extent and the photocurrent often follows the light intensity linearly[63,70,133] or slightly sublinearly.[49,134,135] Though in the bilayer heterojunction the donor and acceptor phase contact the anode and cathode selectively, the bulk heterojunction requires percolated pathways for the hole and electron transporting phases to the contacts. In other words, the donor and acceptor phases have to form a bicontinuous and interpenetrating network. Therefore, the bulk heterojunction devices are much more sensitive to the nanoscale morphology in the blend, which will be discussed in more detail below.

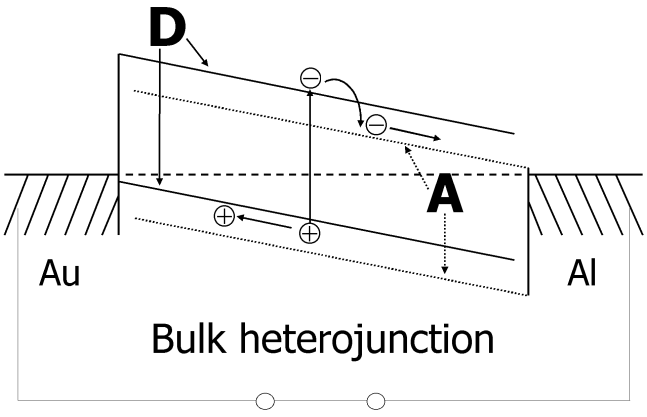

FIG. 11. Schematic of a bulk heterojunction device. The donor (D) is blended with the acceptor (A) throughout the whole film. Thus, photogenerated excitons can be dissociated into charges at any place.

Generally, bulk heterojunctions may be achieved by co-deposition of donor and acceptor pigments[37,67,68,103] or solution casting of either polymer/polymer,[52–54] polymer/molecule,[17,49,50,136,137] or molecule/molecule[138,139] donor–acceptor blends. The most efficient devices today are based on solution cast P3HT:PCBM blends yielding above 3.5% power conversion efficiency under AM 1.5.[64]

D. Diffuse bilayer heterojunction

Another device architecture, which is conceptually in-between the bilayer and the bulk heterojunction device, is the diffuse bilayer heterojunction device. This device structure is aiming to adapt the advantages of both concepts, an enlarged donor–acceptor interface and a spatially uninterrupted pathway for the opposite charge carriers to their corresponding electrodes. The diffuse interface is achieved in different ways: (i) If processed from solution, two thin polymer films can be pressed together in a lamination procedure applying moderate pressure and elevated temperatures.[55] (ii) Another way to achieve a diffuse interface is to spin coat the second layer from a solvent that partially dissolves the underlying polymer layer.[140,141] (iii) Finally, also the controlled interdiffusion between an acceptor fullerene and a donor polymer by annealing of a bilayer device[142] results in an intermixed interfacial region.

Calculated power conversion efficiencies approaching 2% were reported for the laminated polymer:polymer device for simulated AM 1.5 conditions.[55]

VI. UNDERSTANDING THE LIMITS: V_{OC}, I_{SC}, FF, AND RESULTING QUANTUM EFFICIENCY

This section is dedicated to a refined analysis of donor–acceptor photovoltaic devices and their limitations with respect to the power conversion efficiency. Equation (2) states that the power conversion efficiency depends linearly on three factors: open circuit voltage V_{OC}, short-circuit current I_{SC}, and the filling factor FF.

Besides that charge carrier generation at electrodes together with diffusion has a further influence on the V_{OC},[143] the metal-insulator-metal (MIM) model predicts the maximum V_{OC} to be determined by the difference in the work functions of the two electrodes.[26] But experimental data showed deviations from this model for example in the case of gold cathodes, where the V_{OC} exceeded largely the expected difference between the electrode work functions.[144] Fermi level pinning between the

https://doi.org/10.1557/JMR.2004.0252

fullerene and the gold electrode has been accounted for this result. However, this behavior was not found to be universal for all metal cathodes.[145] Hence, the individual energy level alignments between organic–metal interfaces are of high interest.[146–153] For example interfacial dipoles at the electrodes can significantly change the apparent work function of a metal[146,149,150,154,155] and this has been exploited to modify the injection behavior of both electrodes.

The commonly used indium tin oxide (ITO) anode can be modified by plasma etching[156,157] or by coating with a higher work function organic hole transport layer,[158–160] to achieve a better match between the energy levels of the anode and the HOMO of the hole conducting material. But even monolayers of polar molecules were found to modify the work function of ITO by up to 0.9 eV.[161] A commonly applied modification of the cathode is the deposition of a very thin LiF layer between the metal electrode and the organic semiconductor. This was found to improve charge injection in LEDs[162,163] and also resulted in some cases in a higher V_{OC} for organic solar cells.[164,165]

But even aluminum electrodes may form a thin layer of oxidized species at the interface to the organic materials, which was identified recently using dynamic time-of-flight secondary ion mass spectrometry.[166,167] All these interfacial effects may change the resulting work function of the electrodes.

In experiments on polymer/fullerene bulk heterojunctions, the open circuit voltage was found to depend strongly on the LUMO of the acceptor[141] as well as on the HOMO of the donor.[168] Generally, the energy difference between the charge transporting states cannot exceed the acceptor LUMO and donor HOMO gap, thus limiting the splitting of the quasi–Fermi levels. In addition, a dependence of the V_{OC} on the fullerene content in the bulk heterojunction blend was observed,[169–172] which was explained by the partial coverage of the cathode by the fullerene.[170] Other experiments show that changing the electrode work function on either side also influences the V_{OC}.[145,173]

A different situation was found in polymer/polymer bilayer devices, where it was shown that the open circuit voltage exceeds the difference in electrode work functions drastically and even in the case of symmetric metal contacts the device exhibited an open circuit voltage as large as 0.7 volts.[174,175] The authors explained this excess voltage by a diffusion current of charge carriers from the bilayer interface toward the contacts, which had to be balanced by the applied V_{OC}. But still a direct dependence of the V_{OC} on the difference in the electrode work functions was observed. Furthermore, the dependence of the charge transport levels on temperature[134,135,176] and light intensity[9,52,135,174,176,177] are reflected in the observed V_{OC}s. In conclusion, the open circuit potential is a sensitive function of the materials' energy levels as well as the engineering of interfaces and contacts.

To maximize short-circuit photocurrents I_{SC} at a given absorption spectrum, it is necessary to understand the optical absorption profile within the active layer of the device. Hence, optical modeling of coherent light propagation was applied to thin layer devices.[9,21,101,178,179] Due to interference effects therein, the maximum photocurrent for a bilayer device was found when the donor–acceptor interface was put at the maximum of the optical electric-field intensity (Fig. 12). With optical modeling, exciton diffusion ranges[9,21,23] and the thickness of the active region[101] were calculated for bilayer devices. In the case of bulk heterojunction solar cells, absorption throughout the whole photoactive layer can contribute to the photocurrent, due to the efficient exciton dissociation everywhere in the bulk.[69,178,180] If the fraction of the absorbed light is known for the whole absorption spectrum, internal quantum efficiencies (IQE) can be deduced. In the case of MDMO-PPV:PCBM, thus an IQE of about 83% could be derived.[178] However, for P3HT:PCBM devices, even an IQE approaching unity was reported.[63]

If I_{SC} coincides with the calculated number of absorbed photons (IQE = 1), an increase in layer thickness may lead to a further increase in the photocurrent (Fig. 13). Nevertheless, the maximum gain for the net photocurrent may be achieved by applying materials with a lower optical band-gap, allowing absorption on a

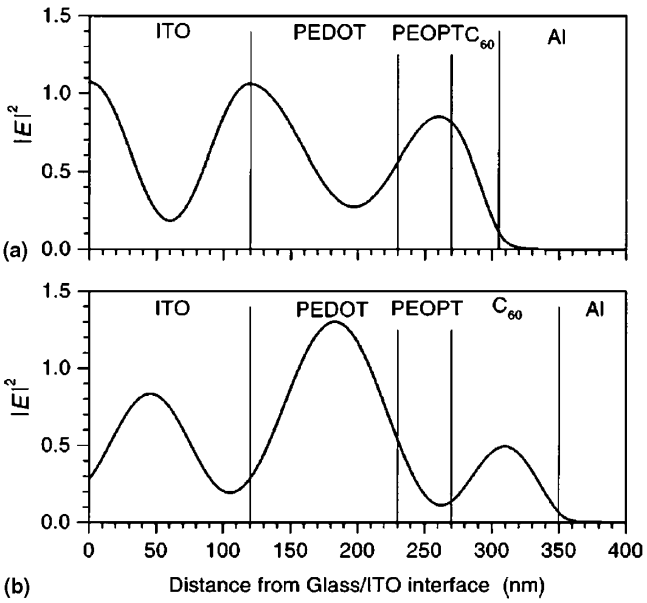

FIG. 12. Calculated distribution of the optical electric-field intensity inside a bilayer donor–acceptor (D-A) device. Two cases are shown: (a) the optimized C_{60} layer thickness with maximal absorption at the donor–acceptor interface, and (b) an unfavorable C_{60} layer thickness resulting in a much smaller absorption. (Reprinted with permission from Ref. 21. Copyright 1999, American Institute of Physics.)

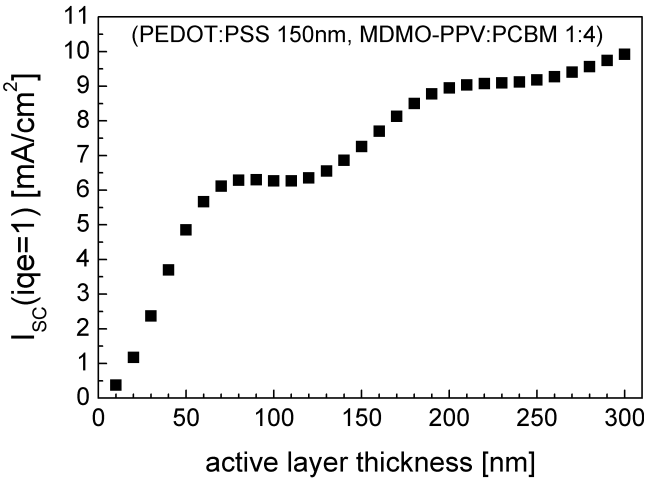

FIG. 13. Calculated photocurrent of a MDMO-PPV:PCBM–based solar cell under the ideal assumption of an internal quantum efficiency of unity. The optical modeling gives upper limits for the achievable photocurrents. The wavy progression is resulting from interference effects. (Reprinted from Ref. 178 with permission from Elsevier. Copyright 2003.)

broader spectral range. Upon exchanging the absorber MDMO-PPV with P3HT, the photocurrents in bulk heterojunction cells can be increased by a factor of two, which is partly due to the lower band gap of regioregular P3HT compared to MDMO-PPV (Fig. 4).

Experimentally it is found that the short-circuit current increases upon increasing the temperature in the polymer/fullerene bulk heterojunction devices.[134,135,176] This indicates a thermally activated hopping transport in these disordered systems.[124] Therefore, the short-circuit photocurrent also depends on the charge-carrier mobility. Organic semiconductors generally are materials exhibiting low mobilities, ranging between $\mu \approx 10^{-5}$ to 10^0 cm^2/Vs.[15] This directly limits the active layer thickness of organic photovoltaic devices. Beyond a certain thickness, the charge carriers will not reach the electrodes before recombination. Therefore, high mobility/low band gap materials are the general route for improving the short circuit current.

The filling factor FF is determined by the fraction of the photogenerated charge carriers that actually reach the electrodes, when the built-in field is lowered toward the open circuit voltage. In fact there is a competition between charge carrier recombination and transport. Hence, the product of the lifetime τ times the mobility μ determines the distance d that charge carriers can drift under a certain electric field E[177]

$$d = \mu \times \tau \times E \quad .$$

To achieve large filling factors, the product $\mu \times \tau$ has to be maximized. If d is approximately equal to the active layer thickness under short-circuit conditions, then the extracted photocurrent shows a stronger dependence on the applied electric field, thus leading to a smaller FF. On the other hand, a large $\mu \times \tau$ product allows to increase the active layer thickness to gain increased absorption and hence I_{SC}, until the FF limits again the overall power efficiency.[181] Furthermore, as stated above, the series resistances influence the filling factor considerably. For example, due to the finite conductivity of the ITO substrate there is a clear dependence of the FF on the active area observed (Ref. 69). To ultimately overcome this, new concepts for higher conductive semitransparent substrates have to be introduced. Finally, the device should be free of "shorts" to maximize the parallel shunt resistance. In conclusion, there is a subtle interplay between the factors determining the efficiency and they have to be resolved together.

VII. CONCEPTS FOR IMPROVEMENT

In this section, some of the recent approaches to improve the overall power conversion efficiency are reviewed. The two main approaches can be identified as either modification of the photoactive layer itself or introduction of transport/blocking layers for an improvement of the contacts.

A. Device engineering and improved charge transport

As already pointed out above, the injection and photovoltage critically depend on the interfaces with the electrodes. Generally, the contact resistance becomes smaller, the smaller the injection barriers at either electron or hole collecting electrodes are. Interfacial layers are often proposed for the lowering of these barriers as shown by the insertion of an ultrathin (<1 nm) layer of LiF between the metal cathodes and the organic semiconductor in LED type devices,[162,163] which resulted in a lower cathode work funtion.[182,183] LiF also improved the contact efficiency in the polymer/fullerene bulk heterojunction solar cells.[164] On the other side, the ITO work function could be increased by plasma treatments[156,157] or by molecular monolayer modifications.[161] The introduction of a layer of PEDOT:PSS (poly[3,4-(ethylenedioxy)-thiophene]:poly(styrene sulfonate),[158,159] a molecularly doped conjugated polymer with a higher work function than ITO,[160] improved organic solar cell performance.[4,48,55,56,103] PEDOT:PSS behaves like a metal[184,185] and its conductivity can reach comparatively high values, also depending on the state of doping and morphological control by solvent treatment and annealing.[186,187] An often applied device structure for polymer/fullerene solar cells is depicted in Fig. 14.

Because metal electrodes are suspected to quench excitons in C60,[188] exciton-blocking layers were introduced in devices between the metal cathode and the C60 layer.[35,179] Additionally, these transparent spacer layers

https://doi.org/10.1557/JMR.2004.0252

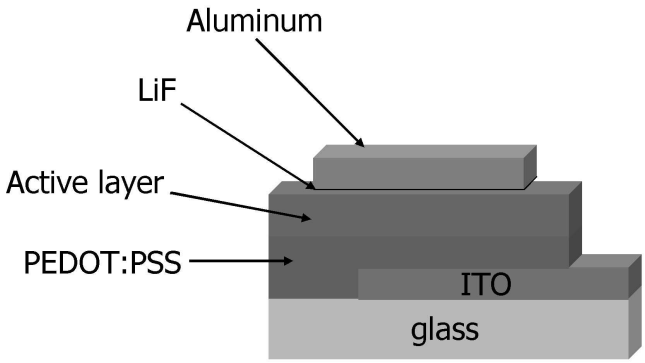

FIG. 14. Optimized device structure for polymer/fullerene bulk heterojunction solar cells. The active layer is sandwiched between the hole transport layer PEDOT:PSS and the LiF modified aluminum cathode.

allow to shift the active layer toward the maximum of the electric-field intensity distribution of the light in these devices.[9,69,179]

Another promising approach is the adaptation of the *p-i-n* concept (known from inorganic solar cells) to organic devices.[38,69,70,102,103] In Fig. 15, the structure and the energy level scheme under short-circuit conditions of a *p-i-n*-solar cell are depicted. Here, an intrinsic organic D-A bulk heterojunction layer is sandwiched between two doped and therefore highly conductive electron transport and hole transport layers. The selectivity of such transport layers provides a good rectification. This *p-i-n* structure compares to the concept of an "ideal solar cell."[189]

The tandem concept offers an interesting approach to increase the open circuit voltage, using a serial connection of two individual *p/n* or *p-i-n* stacked solar cells.[36,69,104,190] One advantage of the tandem cell occurs when the active region within a D-A junction is (due to a series resistance limitation) too thin for efficient absorption in a single layer; in such cases application of multilayers may compensate for this. Practically, the opposite charges generated within the two inner photoactive layers have to recombine at the interface between both cells to achieve voltage doubling. It is found that metal clusters lead to an enhanced recombination,[36,69,190] which was partially assigned to the image charge effect.[190] In the *p-i-n* solar cells, this recombination occurs very selectively, provided by the specific electron and hole transport layers.[69,104] Because the solar cells are serially connected in the tandem structure, the currents of both single cells have to be matched. To achieve this, optical modeling is used as a tool to balance the absorption in both cells.

B. Increasing the absorption range

Because most of the available conjugated polymers were originally developed for visible-light-emitting diodes, they exhibit band gaps ⩾2 eV. Hence, there is a clear mismatch between the absorption spectrum of these materials and the terrestrial solar spectrum, which extends into the near infrared (Fig. 4). Light-trapping geometries were successfully applied, however without a considerable increase in the absorption toward the near infrared part of the solar spectrum.[35,191,192] As external quantum efficiencies of optimized polymer/fullerene solar cells currently exceed 70% at the absorption peak[63,64] and approach unity for internal quantum efficiencies,[59,63,178] the only way to substantially increase the solar photon harvesting is to introduce low band gap materials.[14,193–196] Hence, new materials with absorption extending to the 800–900 nm regime are needed for efficient photon harvesting.

Another approach is to increase the absorption of the fullerene, which was recently demonstrated upon replacing C_{60}-PCBM with C_{70}-PCBM.[66] Due to the increased absorption of the C_{70} methano-fullerene in the visible, the external quantum efficiency (EQE) was increased when compared to the same blend prepared from C_{60} based PCBM.

Because it proved rather difficult to develop suitable organic low-band gap materials, the introduction of inorganic nanocrystals is another possible route to increase the visible absorption. Broad range absorbing copper

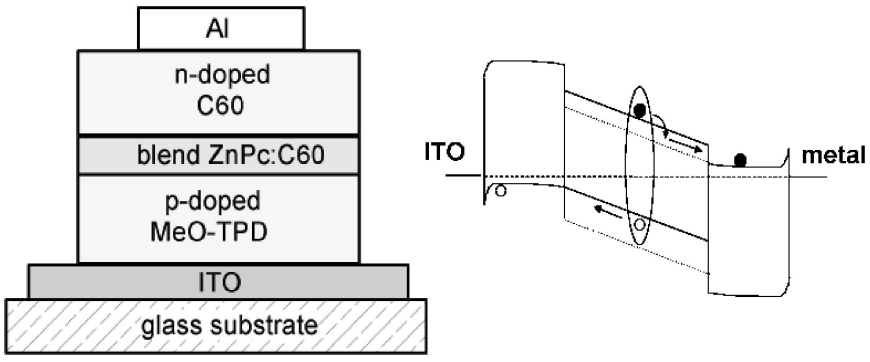

FIG. 15. The structure (left) and the energetic description at closed circuit conditions (right) of an organic *p-i-n* solar cell is shown. The wide-gap *p*-doped hole (MeO-TPD) and *n*-doped electron (C_{60}) transport layers provide good contacts with the electrodes. (Drawings courtesy of M. Pfeiffer, IAPP, TU Dresden.)

https://doi.org/10.1557/JMR.2004.0252

indium disulphide $CuInS_2$ (CIS) nanoparticles were used, and the spectral photocurrent indeed was extended up to 900 nm.[91] However, each of these spectral photon-harvesting approaches involves new material synthesis and an optimization of the nanomorphology in the solid blends has to be carried out for every new material combination.

VIII. INFLUENCE OF THE NANOSCALE MORPHOLOGY

The requirement of an intimate intermixing of donor and acceptor phases in the bulk heterojunction makes this approach especially sensitive to the nanoscale morphology.

To control the size of fullerene domains in a polythiophene/C_{60} bulk heterojunction, a plasticizer additive was applied.[197] The plasticizer consisted of two molecular parts, one interacting with the polymer and the other with the C_{60}. Thus, the intention was to increase the miscibility of both materials, leading to finer phase segregation. Indeed, this yielded a more even distribution of fullerene clusters within the polythiophene matrix. Recently, it was demonstrated that a strong increase in power conversion efficiency was achieved upon changing the casting solvent used for spin coating MDMO-PPV:PCBM bulk heterojunctions.[59] Because the absorption spectrum was not affected, the improvement had to come from a change in the nanoscale morphology of the donor–acceptor mixture. For solvent processed systems, there is a strong dependence of the final morphology on the specific solvent used,[59,66,170,198] solvent evaporation time,[199,200] surface interactions,[201] and postproduction annealing.[64,136,137,139,202] In vacuum evaporated molecular systems, the final morphology depends on the evaporation rate, substrate temperature,[67,203] and also on postproduction annealing.[68] Obviously, the D-A composition is another factor determining the resulting morphology.[172,204,205] The main processes directly affected by the morphology are the exciton diffusion and subsequent dissociation (η_{diss}) as well as the charge transport to the electrodes (η_{out}). Therefore, the morphology has a strong impact on the overall solar cell performance, as will be discussed in the next section.

A. Optimizing the bulk heterojunction nanomorphology

To achieve high quantum efficiency, all photogenerated excitons have to reach and dissociate at a donor–acceptor interface, and subsequently all created charges have to reach the respective electrodes.

Photoluminescence quenching[9,20] and photocurrent modeling[9,21,23] indicate that only photogenerated excitons in proximity to the D-A interface within less than the exciton diffusion length can be dissociated. To ensure the most intimate mixing, D-A dyads[206–210] and D-Apolymers (double cables)[211,212] were synthesized and used as photoactive materials in organic solar cells. However, power conversion efficiencies of solar cells using such covalently attached donor–acceptor supramolecules are rather low, indicating loss mechanisms due to enhanced recombination and poor charge-carrier transport. This leads to the conclusion, that too intimate mixing may result in too small mean free paths. Thus, the critical issue will not only be the relationship between molecular structure and device properties but also between nanomorphology and device properties (Fig. 16).

The use of toluene as solvent in the MDMO-PPV:PCBM system led to a coarser phase separation (~200–500-nm grain size) than for chlorobenzene (~50-nm grain size). This was shown with AFM[59] and transmission electron microscopy (TEM) measurements on this system.[204] Scanning electron microscopy (SEM) measurements show that the polymer phase exhibited a domain size of about 20 nm.[172] Two cross-section SEM images of MDMO-PPV:PCBM spin cast films are shown in Fig. 17 for comparison. The large-scale phase separation in the case of toluene as well as the 20 nm-sized polymeric nanospheres are clearly visible. The larger scale phase separation yielded smaller photocurrents, and unquenched photoluminescence from PCBM could be detected.[172] This photoluminescence could be attributed to the large fullerene clusters in the film. Hence, the phase separation length scale in the toluene case was too large for the dissociation of all photogenerated excitons in the PCBM and this lowered the photocurrent. In contrast, when using chlorobenzene as solvent, no photoluminescence of PCBM could be detected. The most efficient devices reported are based on chlorobenzene and have a large fullerene content of up to 80% by weight.[59–62] Field-effect mobility measurements for different blends of MEH-PPV and PCBM showed increased electron mobility upon increasing the fullerene content (Fig. 18).[117] Similar trends have been found for the MDMO-PPV:PCBM system.[116] Therefore, the high PCBM load is needed for an efficient electron transport, indicating that a minimum grain size of the PCBM acceptor phase may be necessary to ensure percolated pathways for the electrons.

This requirement is in accordance with recent measurements on a small molecule system[68] and others.[136,137] It was found that upon annealing, an initially fine phase separation was coarsening, resulting in better charge transport properties in the bulk heterojunction.

When these results are considered together, they suggest that an optimum domain size of the phase separation between donor and acceptor is needed, to balance exciton dissociation and charge transport requirements.

The temperature controlled nanomorphology leads to the question on how stable the bulk heterojunctions are

https://doi.org/10.1557/JMR.2004.0252

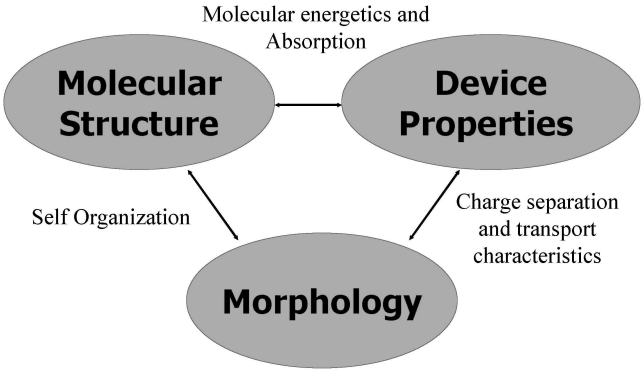

FIG. 16. In organic or hybrid bulk heterojunction solar cells, the molecular structure, nanoscale morphology, and device properties are closely interrelated. Hence, the design of advanced organic solar cells requires the simultaneous optimization of these closely interconnected parameters.

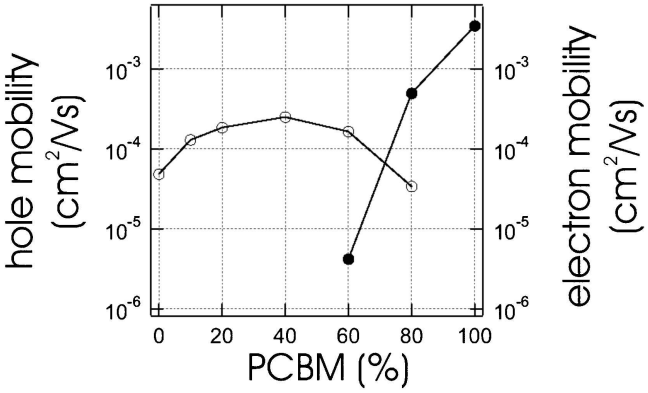

FIG. 18. Hole and electron mobility calculated from FET measurements in blends of MEH-PPV and PCBM of different proportions. A very strong dependence of the electron mobility on the PCBM content is found. The hole mobility in the blend exceeds that of pristine MEH-PPV for a PCBM content of up to 70%. (Reprinted from Ref. 116 with permission.)

against aging effects. Annealing experiments at roughly 150 °C resulted in micrometer sized PCBM aggregates within a few hours, driven by the diffusion and crystallization of PCBM.[172] On the other hand, the performance of P3HT:PCBM devices were found to depend on the time of postproduction annealing: after an initial increase, the efficiency drops on the scale of several minutes.[64] The initial increase may be a result of enlarged PCBM domains in the blend, leading to improved electron transport properties of the device, whereas further annealing results in morphological degradation due to too large PCBM domains. Hence, morphological stability in organic solar cells is an issue to be addressed, as under operating conditions elevated temperatures must be expected. In conclusion, the optimal morphology of a bulk heterojunction device requires stable, nanometer-sized interpenetrating donor and acceptor domains.

B. Concepts for nanomorphology control

A-B diblock-copolymers are known to exhibit self-organized structures depending on the fractions of A and B.[213] The resulting stable phase separated structures are on the scale of the respective block lengths and thus the domain sizes can be controlled down to the nanometer scale. First applications of these self-assembling diblock-copolymers in organic solar cells have been demonstrated.[214,215] The polymer structure is depicted in Fig. 19 resulting in the formation of a honeycomb structure on the micrometer scale. Though this approach included pendant fullerenes in the acceptor block, other acceptor block structures based on *n*-type conjugated polymers were reported recently.[216]

In another approach, it was recently demonstrated that nanometer-sized polymer spheres could be obtained via a miniemulsion preparation (Fig. 20).[217] Polymer particles were stabilized in aqueous dispersion using surfactants under the influence of ultrasonication. Subsequently, these nanoparticles could be spin cast into thin films. This technique was applied to fabricate solar cells with different polyfluorenes as donor and acceptor. The performance of these devices was only dependent on the nanoparticle size, in contrast to solar cells with active layers spin cast from a mixture of the same polymers,

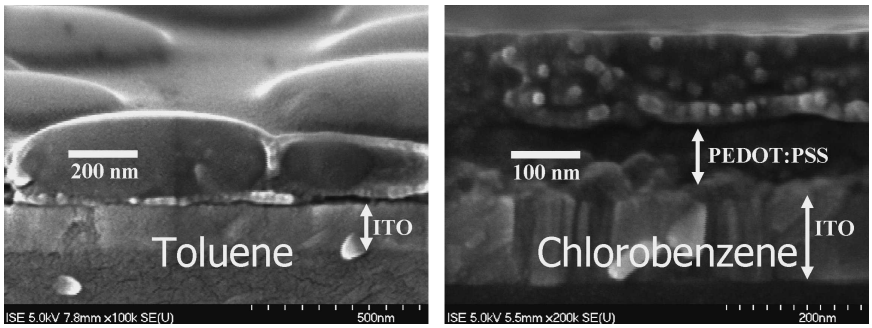

FIG. 17. Scanning electron measurements of break sections of MDMO-PPV:PCBM blend films spin-cast from two different solvents onto ITO(/PEDOT:PSS) covered glass. Clearly, the toluene results in a much coarser phase separation than the chlorobenzene. The observed nanospheres of approximately 10 nm radius can be attributed to the polymer in both cases. (Reproduced from Ref. 172 with permission of Wiley-VCH, Weinheim, Germany.)

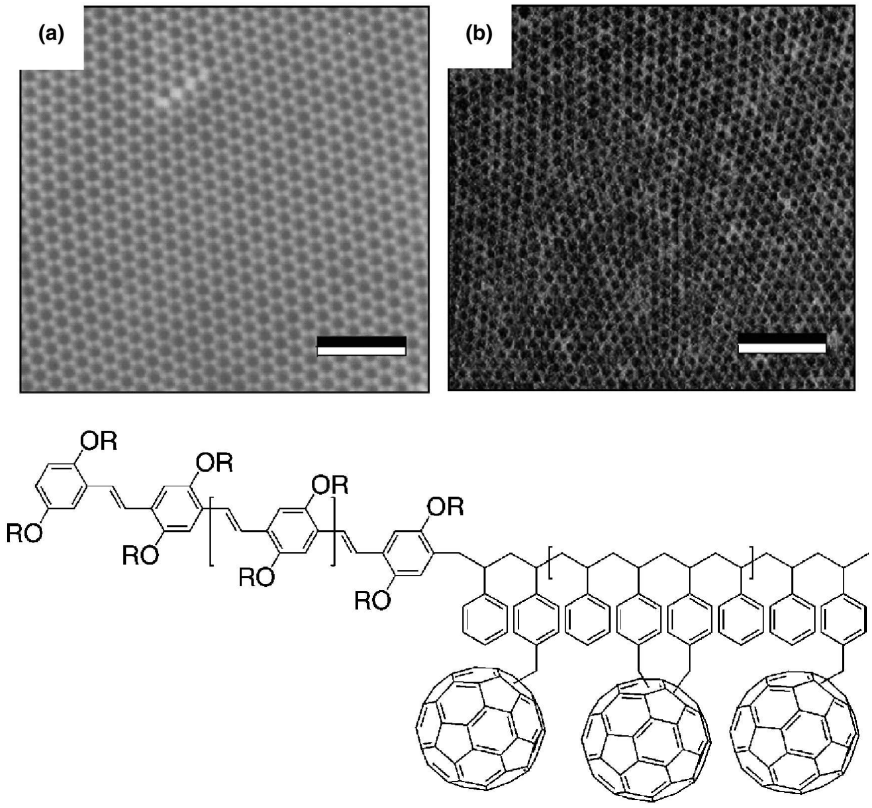

FIG. 19. Luminescence micrographs showing the honeycomb structure of thin films of di-block copolymers as shown below (scale bars: 20 μm). In (a), the local photoluminescence (PL) of a structure without the fullerenes is compared with (b) the one including pendant fullerenes, where a strong PL-quenching is observed. (Reproduced from Ref. 215 by permission of *MRS Bulletin*.)

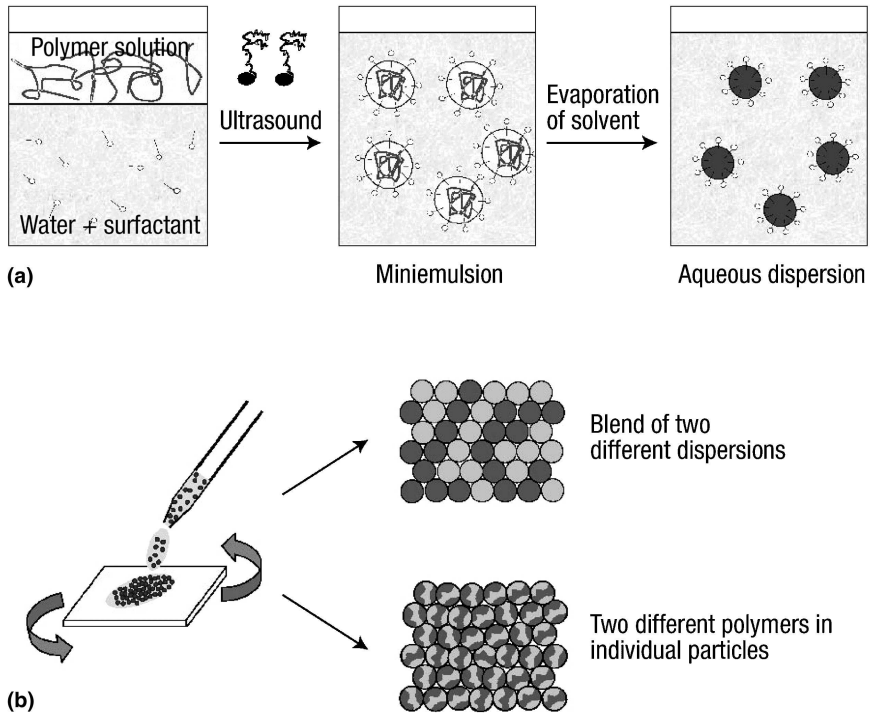

FIG. 20. (a) The production of polymer nanoparticles via a mini-emulsion route. (b) The polymer nanoparticles can be spin cast from aqueous dispersion into thin films. The morphology of the film can be controlled by blending different polymers after or before the mini-emulsion process. (Reproduced from Ref. 217 with permission of the Nature Publishing Group; http://www.nature.com.)

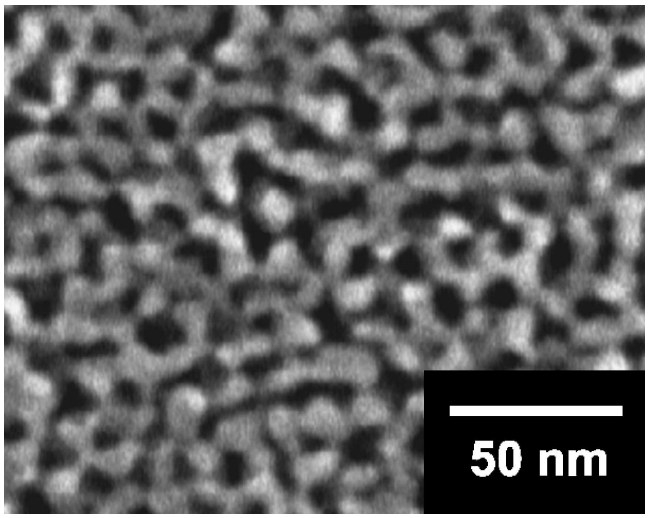

FIG. 21. Scanning electron micrograph of a mesoporous TiO_2 film, obtained by calcination of a precursor. The pores of these nanostructured electrodes were filled with P3HT by spin coating. This method gives high control over the pore size and thus the scale of phase separation. (Reprinted with permission from Ref. 219. Copyright 2003, American Institute of Physics.)

where the quantum efficiency depended strongly on the solvent used. The advantage of this procedure is the ability to produce polymer nanoparticles of desired size as a first step towards controlling of the nanoscopic domain size in the blend.

Other approaches include the application of inorganic nanostructures. Based on a preparation route applying tri-block-copolymers as structure directing agents, regular nanoporous TiO_2 structures could be obtained by calcination of a precursor-film (Fig. 21).[218,219] Then, the nanopores were filled with a donor type (P3HT) semiconducting polymer, spin cast on top of the structure followed by an annealing step. This approach allows a precise control of the interfacial structure within hybrid solar cells.

Finally, the application of inorganic nanoparticles (e.g., CdSe) as acceptor materials in a blend with P3HT (Fig. 22) resulted in maximum EQEs of about 55% and solar power conversion efficiencies approaching 2%.[73] The synthesis of these nanoparticles allows a high degree of control over size and shape.[220] Thus, the acceptor domain size can be tuned to optimize exciton dissociation and electron transport . In these organic–inorganic hybrid bulk heterojunctions, the miscibility of the two phases is critical. Inorganic nanoparticles are generally coated with an organic ligand, the properties of which can be used to facilitate the intermixing of the inorganic nanoparticles with the organic matrix.[221]

IX. CONCLUSIONS AND OUTLOOK

Donor–acceptor based organic solar cells are currently showing power conversion efficiencies of more than 3.5%. Improving the nanoscale morphology together with the development of novel low bandgap materials is expected to lead to power conversion efficiencies approaching 10%. The flexible, large-area applications of organic solar cells may open up new markets like "textile integration." Organic semiconductor devices in general and organic solar cells in particular can be integrated into production lines of packaging materials, labels, and so forth. Because there is a strong development effort for organic electronics integration into different products

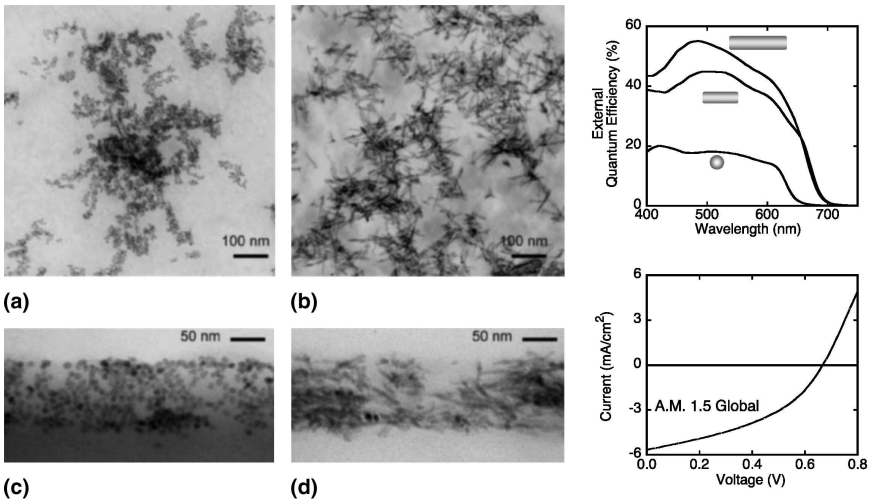

FIG. 22. Hybrid (organic/inorganic) solar cells based on CdSe nanocrystals and P3HT. On the left, transmission electron micrographs showing film morphologies for circular and rod-shaped nanocrystals are depicted (a, b: top view; c, d: cross section). The external quantum efficiencies of these devices exhibit a clear dependence on the aspect ratio of the CdSe nanocrystals. The rod-like nanocrystals yielded higher efficiencies, probably due to a better and more directed charge transport within these rods. (Excerpted with permission from Ref. 73. Copyright 2002, American Association for the Advancement of Science; http://www.sciencemag.org.)

worldwide, the solar powering of some of these products will be desired. The next generation of microelectronics is aiming for applications of "electronics everywhere," and such organic semiconductors will play a major role in these future technologies. Combinations of organic solar cells with batteries, fuel cells, and so forth, will enhance their product integration. This integrability of organic solar cells into many products will be their technological advantage.

ACKNOWLEDGMENTS

We thank M. Pfeiffer, J. Drechsel, R. Koeppe, and M. Scharber for useful discussions, and C. Winder for providing the chemical structures.

REFERENCES

1. A. Goetzberger, C. Hebling, and H-W. Schock: Photovoltaic materials, history, status and outlook. *Mater. Sci. Eng. R* **40,** 1 (2003).
2. G.A. Chamberlain: Organic solar cells: A review. *Solar Cells* **8,** 47 (1983).
3. D. Wöhrle and D. Meissner: Organic solar cells. *Adv. Mater.* **3,** 129 (1991).
4. C.J. Brabec, N.S. Sariciftci, and J.C. Hummelen: Plastic solar cells. *Adv. Funct. Mater.* **11,** 15 (2001).
5. J.J.M. Halls and R.H. Friend: in *Clean Electricity from Photovoltaics*, edited by M.D. Archer and R. Hill (Imperial College Press, London, U.K., 2001).
6. J. Nelson: Organic photovoltaic films. *Curr. Opin. Solid State Mater. Sci.* **6,** 87 (2002).
7. J-M. Nunzi: Organic photovoltaic materials and devices. *C. R. Physique* **3,** 523 (2002).
8. *Organic Photovoltaics: Concepts and Realization*; *Vol. 60*, edited by C.J. Brabec, V. Dyakonov, J. Parisi, and N.S. Sariciftci (Springer, Berlin, Germany, 2003).
9. P. Peumans, A. Yakimov, and S.R. Forrest: Small molecular weight organic thin-film photodetectors and solar cells. *J. Appl. Phys.* **93,** 3693 (2003).
10. *Handbook of Conducting Polymers, Vol. 1-2*, edited by T.A. Skotheim (Marcel Dekker, Inc., New York, 1986).
11. *Handbook of Organic Conductive Molecules and Polymers, Vol. 1-4*, edited by H.S. Nalwa (John Wiley & Sons Ltd., Chichester, U.K., 1997).
12. *Handbook of Conducting Polymers*, edited by T.A. Skotheim, R.L. Elsenbaumer, and J.R. Reynolds (Marcel Dekker, Inc., New York, 1998).
13. *Semiconducting Polymers,* edited by G. Hadziioannou and P.F. van Hutten (Wiley-VCH, Weinheim, 2000).
14. C. Winder and N.S. Sariciftci: Low Bandgap polymers for photon harvesting in bulk heterojunction solar cells. *J. Mater. Chem.* **14,** 1077 (2004).
15. C.D. Dimitrakopoulos and D.J. Mascaro: Organic thin-film transistors: A review of recent advances. *IBM J. Res. Dev.* **45,** 11 (2001).
16. J.J.M. Halls, K. Pichler, R.H. Friend, S.C. Moratti, and A.B. Holmes: Exciton diffusion and dissociation in a poly(p-phenylenevinylene)/C60 heterojunction photovoltaic cell. *Appl. Phys. Lett.* **68,** 3120 (1996).
17. J.J.M. Halls and R.H. Friend: The photovoltaic effect in a poly(p-phenylenevinylene)/perylene heterojunction. *Synth. Met.* **85,** 1307 (1997).
18. H.R. Kerp, H. Donker, R.B.M. Koehorst, T.J. Schaafsma, and E.E. van Faassen: Exciton transport in organic dye layers for photovoltaic applications. *Chem. Phys. Lett.* **298,** 302 (1998).
19. T.J. Savanije, J.M. Warman, and A. Goossens: Visible light sensitisation of titanium dioxide using a phenylene vinylene polymer. *Chem. Phys. Lett.* **287,** 148 (1998).
20. A. Haugeneder, M. Neges, C. Kallinger, W. Spirkl, U. Lemmer, J. Feldmann, U. Scherf, E. Harth, A. Gügel, and K. Müllen: Exciton diffusion and dissociation in conjugated polymer/fullerene blends and heterostructures. *Phys. Rev. B* **59,** 15346 (1999).
21. L.A.A. Pettersson, L.S. Roman, and O. Inganäs: Modeling photocurrent action spectra of photovoltaic devices based on organic thin films. *J. Appl. Phys.* **86,** 487 (1999).
22. M. Stoessel, G. Wittmann, J. Staudigel, F. Steuber, J. Blässing, W. Roth, H. Klausmann, W. Rogler, J. Simmerer, A. Winnacker, M. Inbasekaran, and E.P. Woo: Cathode-induced luminescence quenching in polyfluorenes. *J. Appl. Phys.* **87,** 4467 (2000).
23. T. Stübinger and W. Brütting: Exciton diffusion and optical interference in organic donor–acceptor photovoltaic cells. *J. Appl. Phys.* **90,** 3632 (2001).
24. Primary Photoexcitations in Conjugated Polymers: Molecular Exciton versus Semiconductor Band Model; edited by N.S. Sariciftci (World Scientific, Singapore, 1997).
25. B.A. Gregg and M.C. Hanna: Comparing organic to inorganic photovoltaic cells: Theory, experiment, and simulation. *J. Appl. Phys.* **93,** 3605 (2003).
26. I.D. Parker: Carrier tunneling and device characteristics in polymer light-emitting diodes. *J. Appl. Phys.* **75,** 1656 (1994).
27. A.K. Gosh, D.L. Morel, T. Feng, R.F. Shaw, and C.A. Rowe, Jr.: Photovoltaic and rectification properties of Al/Mg phthalocyanine/Ag Schottky-barrier cells. *J. Appl. Phys.* **45,** 230 (1974).
28. D. Meissner, S. Siebentritt, and S. Günster: *Charge carrier photogeneration in organic solar cells,* presented at the International Symposium on Optical Materials Technology for Energy Efficiency and Solar Energy Conversion XI: Photovoltaics, Photochemistry and Photoelectrochemistry, Toulouse, France, 1992.
29. S. Karg, W. Riess, V. Dyakonov, and M. Schwoerer: Electrical and optical characterization of poly(phenylene-vinylene) light emitting diodes. *Synth. Met.* **54,** 427 (1993).
30. D.L. Morel, A.K. Gosh, T. Feng, E.L. Stogryn, P.E. Purwin, R.F. Shaw, and C. Fishman: High-efficiency organic solar cells. *Appl. Phys. Lett.* **32,** 495 (1978).
31. A.K. Gosh and T. Feng: Merocyanine organic solar cells. *J. Appl. Phys.* **49,** 5982 (1978).
32. S.M. Sze: *Physics of Semiconductor Devices* (John Wiley & Sons, New York, 1981).
33. C.W. Tang: Two-layer organic photovoltaic cell. *Appl. Phys. Lett.* **48,** 183 (1986).
34. J. Rostalski and D. Meissner: Monochromatic versus solar efficiencies of organic solar cells. *Sol. Energy Mater. Sol. Cells* **61,** 87 (2000).
35. P. Peumanns, V. Bulovic, and S.R. Forrest: Efficient photon harvesting at high optical intensities in ultrathin organic double-heterostructure photovoltaic diodes. *Appl. Phys. Lett.* **76,** 2650 (2000).
36. M. Hiramoto, M. Suezaki, and M. Yokoyama: Effect of thin gold interstitial-layer on the photovoltaic properties of tandem organic solar cells. *Chem. Lett.* **19,** 327 (1990).
37. M. Hiramoto, H. Fujiwara, and M. Yokoyama: Three-layered organic solar cell with a photoactive interlayer of codeposited pigments. *Appl. Phys. Lett.* **58,** 1062 (1991).
38. M. Hiramoto, H. Fujiwara, and M. Yokoyama: p-i-n like behavior in three-layered organic solar cells having a co-deposited interlayer of pigments. *J. Appl. Phys.* **72,** 3781 (1992).

39. R.N. Marks, J.J.M. Halls, D.D.C. Bradley, R.H. Friend, and A.B. Holmes: The photovoltaic response in poly(p-phenylene vinylene) thin-film devices. *J. Phys.: Condens. Matter.* **6,** 1379 (1994).
40. G. Yu, C. Zhang, and A.J. Heeger: Dual-function semiconducting polymer devices: Light-emitting and photodetecting diodes. *Appl. Phys. Lett.* **64,** 1540 (1994).
41. H. Antoniadis, B.R. Hsieh, M.A. Abkowitz, S.A. Jenekhe, and M. Stolka: Photovoltaic and photoconductive properties of aluminum/poly(p-phenylene vinylene) interfaces. *Synth. Met.* **62,** 265 (1994).
42. N.S. Sariciftci, L. Smilowitz, A.J. Heeger, and F. Wudl: Photoinduced electron transfer from a conducting polymer to buckminsterfullerene. *Science* **258,** 1474 (1992).
43. L. Smilowitz, N.S. Sariciftci, R. Wu, C. Gettinger, A.J. Heeger, and F. Wudl: Photoexcitation spectroscopy of conducting-polymer-C60 composites: Photoinduced electron transfer. *Phys. Rev. B* **47,** 13835 (1993).
44. C.H. Lee, G. Yu, D. Moses, K. Pakbaz, C. Zhang, N.S. Sariciftci, A.J. Heeger, and F. Wudl: Sensitization of the photoconductivity of conducting polymers by C60: Photoinduced electron transfer. *Phys. Rev. B* **48,** 15425 (1993).
45. S. Morita, A.A. Zakhidov, and K. Yoshino: Doping effect of buckminsterfullerene in conducting polymer: Change of absorption spectrum and quenching of luminescene. *Solid State Commun.* **82,** 249 (1992).
46. S. Morita, S. Kiyomatsu, X.H. Yin, A.A. Zakhidov, T. Noguchi, T. Ohnishi, and K. Yoshino: Doping effect of buckminsterfullerene in poly(2,5-dialkoxy-p-phenylene vinylene). *J. Appl. Phys.* **74,** 2860 (1993).
47. N.S. Sariciftci, D. Braun, C. Zhang, V.I. Srdanov, A.J. Heeger, G. Stucky, and F. Wudl: Semiconducting polymer-buckminsterfullerene heterojunctions: Diodes, photodiodes, and photovoltaic cells. *Appl. Phys. Lett.* **62,** 585 (1993).
48. L.S. Roman, W. Mammo, L.A.A. Petterson, M.R. Andersson, and O. Inganäs: High quantum efficiency polythiophene/C60 photodiodes. *Adv. Mater.* **10,** 774 (1998).
49. G. Yu, J. Gao, J.C. Hummelen, F. Wudl, and A.J. Heeger: Polymer photovoltaic cells: Enhanced efficiencies via a network of internal donor-acceptor heterojunctions. *Science* **270,** 1789 (1995).
50. C.Y. Yang and A.J. Heeger: Morphology of composites of semiconducting polymers mixed with C60. *Synth. Met.* **83,** 85 (1996).
51. J.C. Hummelen, B.W. Knight, F. LePeq, F. Wudl, J. Yao, and C.L. Wilkins: Preparation and characterization of fulleroid and methanofullerene derivatives. *J. Org. Chem.* **60,** 532 (1995).
52. G. Yu and A.J. Heeger: Charge separation and photovoltaic conversion in polymer composites with internal donor/acceptor heterojunctions. *J. Appl. Phys.* **78,** 4510 (1995).
53. J.J.M. Halls, C.A. Walsh, N.C. Greenham, E.A. Marseglia, R.H. Friend, S.C. Moratti, and A.B. Holmes: Efficient photodiodes from interpenetrating polymer networks. *Nature* **376,** 498 (1995).
54. K. Tada, K. Hosada, M. Hirohata, R. Hidayat, T. Kawai, M. Onoda, M. Teraguchi, T. Masuda, A.A. Zakhidov, and K. Yoshino: Donor polymer (PAT6) - acceptor polymer (CN-PPV) fractal network photocells. *Synth. Met.* **85,** 1305 (1997).
55. M. Granström, K. Petritsch, A.C. Arias, A. Lux, M.R. Andersson, and R.H. Friend: Laminated fabrication of polymeric photovoltaic diodes. *Nature* **395,** 257 (1998).
56. P. Peumanns and S.R. Forrest: Very-high-efficiency double-heterostructure copper phthalocyanine/C60 photovoltaic cells. *Appl. Phys. Lett.* **79,** 126 (2001).
57. P. Peumans and S.R. Forrest: Erratum: Very-high-efficiency double-heterostructure copper phthalocyanine/C60 photovoltaic cells. *Appl. Phys. Lett.* **79,** 126 (2001).
58. J. Xue, S. Uchida, B.P. Rand, and S.R. Forrest: 4.2% efficient organic photovoltaic cells with low series resistances. *Appl Phys. Lett.* **84,** 3013 (2004).
59. S.E. Shaheen, C.J. Brabec, N.S. Sariciftci, F. Padinger, T. Fromherz, and J.C. Hummelen: 2.5% efficient organic plastic solar cells. *Appl. Phys. Lett.* **78,** 841 (2001).
60. J.M. Kroon, M.M. Wienk, W.J.H. Verhees, and J.C. Hummelen: Accurate efficiency determination and stability studies of conjugated polymer/fullerene solar cells. *Thin Solid Films* **403–404,** 223 (2002).
61. T. Munters, T. Martens, L. Goris, V. Vrindts, J. Manca, L. Lutsen, W.D. Ceunick, D. Vanderzande, L.D. Schepper, J. Gelan, N.S. Sariciftci, and C.J. Brabec: A comparison between state-of-the-art 'gilch' and 'sulphinyl' synthesised MDMO-PPV/PCBM bulk heterojunction solar cells. *Thin Solid Films* **403–404,** 247 (2002).
62. T. Aernouts, W. Geens, J. Portmans, P. Heremans, S. Borghs, and R. Mertens: Extraction of bulk and contact components of the series resistance in organic bulk donor-acceptor-heterojunctions. *Thin Solid Films* **403,** 297 (2002).
63. P. Schilinsky, C. Waldauf, and C.J. Brabec: Recombination and loss analysis in polythiophene based bulk heterojunction photodetectors. *Appl. Phys. Lett.* **81,** 3885 (2002).
64. F. Padinger, R.S. Rittberger, and N.S. Sariciftci: Effects of post-production treatment on plastic solar cells. *Adv. Funct. Mater.* **13,** 1 (2003).
65. M. Svensson, F. Zhang, S.C. Veenstra, W.J.H. Verhees, J.C. Hummelen, J.M. Kroon, O. Inganäs, and M.R. Andersson: High-performance polymer solar cells of an alternating polyfluorene copolymer and a fullerene derivative. *Adv. Mater.* **15,** 988 (2003).
66. M.M. Wienk, J.M. Kroon, W.J.H. Verhees, J. Knol, J.C. Hummelen, P.A. van Hall, and R.A.J. Janssen: Efficient methano[70]fullerene/MDMO-PPV bulk heterojunction photovoltaic cells. *Angew. Chem. Int. Ed.* **42,** 3371 (2003).
67. W. Geens, T. Aernouts, J. Poortmans, and G. Hadziioannou: Organic co-evaporated films of a PPV-pentamer and C60: Model systems for donor/acceptor polymer blends. *Thin Solid Films* **403,** 438 (2002).
68. P. Peumans, S. Uchida, and S.R. Forrest: Efficient bulk heterojunction photovoltaic cells using small-molecular-weight organic thin films. *Nature* **425,** 158 (2003).
69. B. Maennig, J. Drechsel, D. Gebeyehu, P. Simon, F. Kozlowski, A. Werner, F. Li, S. Grundmann, S. Sonntag, M. Koch, K. Leo, M. Pfeiffer, H. Hoppe, D. Meissner, S. Sariciftci, I. Riedel, V. Dyakonov, and J. Parisi: Organic p-i-n solar cells. *Appl. Phys. A* **79,** 1 (2004).
70. D. Gebeyehu, M. Pfeiffer, B. Maennig, J. Drechsel, A. Werner, and K. Leo: Highly efficient p-i-n type organic photovoltaic devices. *Thin Solid Films* **451–452,** 29 (2004).
71. J. Krüger, R. Plass, L. Cevey, M. Piccirelli, M. Grätzel, and U. Bach: High efficiency solid-state photovoltaic device due to inhibition of interface charge recombination. *Appl. Phys. Lett.* **79,** 2085 (2001).
72. J. Krüger, R. Plass, M. Grätzel, and H-J. Matthieu: Improvement of the photovoltaic performance of solid-state dye-sensitized device by silver complexation of the sensitizer cis-bis(4,4-dicarboxy-2,2bipyridine)-bis(isothiocyanato) ruthenium(II). *Appl. Phys. Lett.* **81,** 367 (2002).
73. W.U. Huynh, J.J. Dittmer, and A.P. Alivisatos: Hybrid Nanorod-Polymer Solar Cells. *Science* **295,** 2425 (2002).
74. H. Tributsch and M. Calvin: Electrochemistry of excited molecules. Photoelectrochemical reactions of chlorophylls. *Photochem. Photobiol.* **14,** 95 (1971).
75. H. Tributsch: Reaction of excited chlorophyll molecules at electrodes and in photosynthesis. *Photochem. Photobiol.* **16,** 261 (1972).
76. T. Osa and M. Fujihira: Photocell using covalently-bound dyes on semiconductor surfaces. *Nature* **264,** 349 (1976).

77. M. Fujihira, N. Ohishi, and T. Osa: Photocell using covalently-bound dyes on semiconductor surfaces. *Nature* **268,** 226 (1977).
78. H. Tsubomura, M. Matsumura, K. Nakatani, K. Yamamoto, and K. Maeda: 'Wet-type' solar cells with semiconductor electrodes. *Sol. Energy* **21,** 93 (1978).
79. M. Matsumura, S. Matsudaira, H. Tsubomura, M. Takata, and H. Yanagida: Sintered ZnO electrode for dye-sensitized photocell. *Yogyo Kyokai Shi* **87,** 167 (1979).
80. B. O'Regan and M. Grätzel: A low cost, high-efficiency solar cell based on dye-sensitized colloidal TiO_2 films. *Nature* **353,** 737 (1991).
81. K. Kalyanasundaram and M. Grätzel: Applications of functionalized transition metal complexes in photonic and optoelectronic devices. *Coordin. Chem. Rev.* **77,** 347 (1998).
82. M. Grätzel: Photoelectrochemical cells. *Nature* **414,** 338 (2001).
83. M. Grätzel: Dye-sensitized solar cells. *J. Photochem. Photobiol. C* **4,** 145 (2003).
84. U. Bach, D. Lupo, P. Comte, J.E. Moser, F. Weissörtel, J. Salbeck, H. Spreitzer, and M. Grätzel: Solid-state dye-sensitized mesoporous TiO_2 solar cells with high photon-to-electron conversion efficiencies. *Nature* **395,** 583 (1998).
85. J.S. Salafsky: Exciton dissociation, charge transport, and recombination in ultrathin, conjugated polymer-TiO_2 nanocrystal intermixed composites. *Phys. Rev. B* **59,** 10885 (1999).
86. A.C. Arango, L.R. Johnson, V.N. Bliznyuk, Z. Schlesinger, S.A. Carter, and H-H. Hörhold: Efficient titanium oxide/conjugated polymer photovoltaics for solar energy conversion. *Adv. Mater.* **89,** 1689 (2000).
87. Q. Fan, B. McQuillin, D.D.C. Bradley, S. Whitelegg, and A.B. Seddon: A solid state solar cell using sol–gel processed material and a polymer. *Chem. Phys. Lett.* **347,** 325 (2001).
88. D. Gebeyehu, C.J. Brabec, F. Padinger, T. Fromherz, S. Spiekermann, N. Vlachopoulos, F. Kienberger, H. Schindler, and N.S. Sariciftci: Solid state dye-sensitized TiO_2 solar cells with poly(3-octylthiophene) as hole transport layer. *Synth. Met.* **121,** 1549 (2001).
89. Y. Saito, T. Kitamura, Y. Wada, and S. Yanagida: Poly(3,4-ethylenedioxythiophene) as a hole conductor in solid state dye sensitized solar cells. *Synth. Met.* **131,** 185 (2002).
90. N.C. Greenham, X. Peng, and A.P. Alivisatos: Charge separation and transport in conjugated-polymer/semiconductor-nanocrystal composites studied by photoluminescence quenching and photoconductivity. *Phys. Rev. B* **54,** 17628 (1996).
91. E. Arici, N.S. Sariciftci, and D. Meissner: Hybrid solar cells based on nanoperticles of $CuInS_2$ in organic matrices. *Adv. Funct. Mater.* **13,** 165 (2003).
92. P.A. van Hal, M.M. Wienk, J.M. Kroon, W.J.H. Verhees, L.H. Slooff, W.J.H. van Gennip, P. Jonkheijm, and R.A.J. Janssen: Photoinduced electron transfer and photovoltaic response of a MDMO-PPV:TiO_2 bulk-heterojunction. *Adv. Mater.* **15,** 118 (2003).
93. M. Pientka, V. Dyakonov, D. Meissner, A. Rogach, D. Talapin, H. Weller, L. Lutsen, and D. Vanderzande: Photoinduced charge transfer in composites of conjugated polymers and semiconductor nanocrystals. *Nanotechnology* **15,** 163 (2004).
94. E. Arici, H. Hoppe, F. Schäffler, D. Meissner, M.A. Malik, and N.S. Sariciftci: Hybrid solar cells based on inorganic nanoclusters and semiconductive polymers. *Thin Solid Films* **451–452,** 612 (2004).
95. E. Arici, N.S. Sariciftci, and D. Meissner: in *Encyclopedia of Nanoscience and Nanotechnology*, edited by H.S. Nalwa (American Scientific Publishers, Stevenson Ranch, CA, 2004).
96. H. Neugebauer, C. Brabec, J.C. Hummelen, and N.S. Sariciftci: Stability and photodegradation mechanisms of conjugated polymer/fullerene plastic solar cells. *Sol. Energy Mater. Sol. Cells* **61,** 35 (2000).
97. F. Padinger, T. Fromherz, P. Denk, C.J. Brabec, J. Zettner, T. Hierl, and N.S. Sariciftci: Degradation of bulk heterojunction solar cells operated in an inert gas atmosphere: A systematic study. *Synth. Met.* **121,** 1605 (2001).
98. C.W. Tang and A.C. Albrecht: Photovoltaic effects of metal-chlorophyll-a-metal sandwich cells. *J. Chem. Phys.* **62,** 2139 (1975).
99. M. Hiramoto, Y. Kishigami, and M. Yokoyama: Doping effect on the two-layer organic solar cell. *Chem. Lett.* **19,** 119 (1990).
100. P.A. Lane, J. Rostalski, C. Giebeler, S.J. Martin, D.D.C. Bradley, and D. Meissner: Electroabsorption studies of phthalocyanine/perylene solar cells. *Sol. Energy Mater. Sol. Cells* **63,** 3 (2000).
101. J. Rostalski and D. Meissner: Photocurrent spectroscopy for the investigation of charge carrier generation and transport mechanisms in organic p/n-junction solar cells. *Sol. Energy Mater. Sol. Cells* **63,** 37 (2000).
102. M. Pfeiffer, A. Beyer, B. Plönnigs, A. Nollau, T. Fritz, K. Leo, D. Schlettwein, S. Hiller, and D. Wöhrle: Controlled p-doping of pigment layers by cosublimation: Basic mechanisms and implication for their use in organic photovoltaic cells. *Sol. Energy Mater. Sol. Cells* **63,** 83 (2000).
103. D. Gebeyehu, B. Maennig, J. Drechsel, K. Leo, and M. Pfeiffer: Bulk-heterojunction photovoltaic devices based on donor-acceptor organic small molecule blends. *Sol. Energy Mater. Sol. Cells* **79,** 81 (2003).
104. J. Drechsel, B. Männig, F. Kozlowski, D. Gebeyehu, A. Werner, M. Koch, K. Leo, and M. Pfeiffer: High efficiency organic solar cells based on single or multiple PIN structures. *Thin Solid Films* **451–452,** 515 (2004).
105. M.S. Dresselhaus, G. Dresselhaus, and P.C. Eklund: *Science of Fullerenes and Carbon Nanotubes* (Academic Press, San Diego, CA, 1996).
106. N.S. Sariciftci and A.J. Heeger: in *Handbook of Organic Conductive Molecules and Polymers*; *Vol. 1*, edited by H.S. Nalwa (John Wiley & Sons Ltd., Chichester, U.K., 1997), p. 413.
107. J.H. Burroughes, D.D.C. Bradley, A.R. Brown, R.N. Marks, K. Mackay, R.H. Friend, P.L. Burns, and A.B. Holmes: Light-emitting diodes based on conjugated polymers. *Nature* **347,** 539 (1990).
108. D. Braun and A.J. Heeger: Visible light emission from semiconducting polymer diodes. *Appl. Phys. Lett.* **58,** 1982 (1991).
109. Organic Light-Emitting Devices: A Survey; edited by J. Shinar (Springer, New York, 2004).
110. D. Adam, P. Schuhmacher, J. Simmerer, L. Häussling, K. Siemensmeyer, K.H. Etzbachi, H. Ringsdorf, and D. Haarer: Fast photoconduction in the highly ordered columnar phase of a discotic liquid crystal. *Nature* **371,** 141 (1994).
111. M. Funahashi and J.-I. Hanna: Fast hole transport in a new calamitic liquid crystal of 2-(4'-heptyloxyphenyl)-6-dodecylthiobenzothiazole. *Phys. Rev. Lett.* **78,** 2184 (1997).
112. H. Sirringhaus, P.J. Brown, R.H. Friend, M.M. Nielsen, K. Bechgaard, B.M.W. Langeveld-Voss, A.J.H. Spiering, R.A.J. Janssen, E.W. Meijer, P. Herwig, and D.M. de Leeuw: Two-dimensional charge transport in self-organized, high-mobility conjugated polymers. *Nature* **401,** 685 (1999).
113. H. Sirringhaus, R.J. Wilson, R.H. Friend, M. Inbasekaran, W. Wu, E.P. Woo, M. Grell, and D.D.C. Bradley: Mobility enhancement in conjugated polymer field-effect transistors through chain alignment in a liquid-crystalline phase. *Appl. Phys. Lett.* **77,** 406 (2000).
114. K.E. Aasmundtveit, E.J. Samuelsen, M. Guldstein, C. Steinsland, O. Flornes, C. Fagermo, T.M. Seeberg, L.A.A. Pettersson, O. Inganäs, R. Feidenhans, and S. Ferrer: Structural anisotropy of poly(alkylthiophene) films. *Macromolecules* **33,** 3120 (2000).
115. U. Zhokhavets, G. Gobsch, H. Hoppe, and N.S. Sariciftci: Anisotropic optical properties of thin poly(3-octylthiophene)-films as a function of preparation conditions. *Synth. Met.* **143,** 113 (2004).

116. W. Geens, S.E. Shaheen, C.J. Brabec, J. Poortmans, and N.S. Sariciftci: Field-effect mobility measurements of conjugated polymer/fullerene photovoltaic blends, presented at the 14th International Winterschool/Euroconference, Kirchberg, Austria, 2000 (AIP).
117. T. Aernouts, P. Vanlaeke, W. Geens, J. Poortmans, P. Heremans, S. Borghs, and R. Mertens: The influence of the donor/acceptor ratio on the performance of organic bulk heterojunction solar cells, presented at the E-MRS Spring Meeting, Strasbourg, France, 2003.
118. S.A. Choulis, J. Nelson, Y. Kim, D. Poplavskyy, T. Kreouzis, J.R. Durrant, and D.D.C. Bradley: Investigation of transport properties in polymer/fullerene blends using time-of-flight photocurrent measurements. *Appl. Phys. Lett.* **83,** 3812 (2003).
119. R. Pacios, J. Nelson, D.D.C. Bradley, and C.J. Brabec: Composition dependence of electron and hole transport in polyfluorene:[6,6]-phenyl C61-butyric acid methyl ester blend films. *Appl. Phys. Lett.* **83,** 4764 (2003).
120. S.C. Veenstra, G.G. Malliaras, H.J. Brouwer, F.J. Esselink, V.V. Krasnikov, P.F. van Hutten, J. Wildeman, H.T. Jonkman, G.A. Sawatzky, and G. Hadziioannou: Sexithiophene-C60 blends as model systems for photovoltaic devices. *Synth. Met.* **84,** 971 (1997).
121. T. Tsuzuki, Y. Shirota, J. Rostalski, and D. Meissner: The effect of fullerene doping on photoelectric conversion using titanyl phthalocyanine and a perylene pigment. *Sol. Energy Mater. Sol. Cells* **61,** 1 (2000).
122. S.E. Shaheen, R. Radspinner, N. Peyghambarian, and G.E. Jabbour: Fabrication of bulk heterojunction plastic solar cells by screen printing. *Appl. Phys. Lett.* **79,** 2996 (2001).
123. B.A. Gregg: Excitonic Solar Cells. *J. Phys. Chem. B* **107,** 4688 (2003).
124. M. Pope and C.E. Swenberg: *Electronic Processes in Organic Crystals and Polymers*, 2nd ed. (Oxford University Press, New York, 1999).
125. M. Murgia, F. Biscarini, M. Cavallini, C. Taliani, and G. Ruani: Intedigitated p-n junction: A route to improve the efficiency in organic photovoltaic cells. *Synth. Met.* **121,** 1533 (2001).
126. G. Ruani, C. Fontanini, M. Murgia, and C. Taliani: Weak intrinsic charge-transfer complexes: A new route for developing wide spectrum organic photovoltaic cells. *J. Chem. Phys.* **116,** 1713 (2002).
127. T. Toccoli, A. Boschetti, C. Corradi, L. Guerini, M. Mazzola, and S. Iannotta: Co-deposition of phthalocyanines and fullerene by SuMBE; Characterization and prototype devices. *Synth. Met.* **138,** 3 (2003).
128. V.I. Arkhipov, P. Heremans, and H. Bässler: Why is exciton dissociation so efficient at the interface between a conjugated polymer and an electron acceptor? *Appl. Phys. Lett.* **82,** 4605 (2003).
129. G. Zerza, C.J. Brabec, G. Cerullo, S.D. Silvestri, and N.S. Sariciftci: Ultrafast charge transfer in conjugated polymer-fullerene composites. *Synth. Met.* **119,** 637 (2001).
130. A.F. Nogueira, I. Montari, J. Nelson, J.R. Durrant, C. Winder, N.S. Sariciftci, and C. Brabec: Charge recombination in conjugated polymer/fullerene blended films studied by transient absorption spectroscopy. *J. Phys. Chem. B* **107,** 1567 (2003).
131. A.J. Breeze, A. Salomon, D.S. Ginley, B.A. Gregg, H. Tillmann, and H-H. Hörhold: Polymer-perylene diimide heterojunction solar cells. *Appl. Phys. Lett.* **81,** 3085 (2002).
132. S.A. Jenekhe and S. Yi: Efficient photovoltaic cells from semiconducting polymer heterojunctions. *Appl. Phys. Lett.* **77,** 2635 (2000).
133. T. Yohannes, F. Zhang, M. Svensson, J.C. Hummelen, M.R. Andersson, and O. Inganäs: Polyfluorene copolymer based bulk heterojunction solar cells. *Thin Solid Films* **449,** 152 (2004).
134. E.A. Katz, D. Faiman, S.M. Tuladhar, J.M. Kroon, M.M. Wienk, T. Fromherz, F. Padinger, C.J. Brabec, and N.S. Sariciftci:Temperature dependence for the photovoltaic device parameters of polymer-fullerene solar cells under operating conditions. *J. Appl. Phys.* **90,** 5343 (2001).
135. V. Dyakonov: The polymer-fullerene interpenetrating network: One route to a solar cell approach. *Physica E* **14,** 53 (2002).
136. J.J. Dittmer, R. Lazzaroni, P. Leclere, P. Moretti, M. Granström, K. Petritsch, E.A. Marseglia, R.H. Friend, J.L. Bredas, H. Rost, and A.B. Holmes: Crystal network formation in organic solar cells. *Sol. Energy Mater. Sol. Cells* **61,** 53 (2000).
137. J.J. Dittmer, E.A. Marseglia, and R.H. Friend: Electron trapping in dye/polymer blend photovoltaic cells. *Adv. Mater.* **12,** 1270 (2000).
138. K. Petritsch, J.J. Dittmer, E.A. Marseglia, R.H. Friend, A. Lux, G.G. Rozenberg, S.C. Moratti, and A.B. Holmes: Dye-based donor/acceptor solar cells. *Sol. Energy Mater. Sol. Cells* **61,** 63 (2000).
139. L. Schmidt-Mende, A. Fechtenkötter, K. Müllen, E. Moons, R.H. Friend, and J.D. MacKenzie: Self-organized discotic liquid crystals for high-efficiency organic photovoltaics. *Science* **293,** 1119 (2001).
140. L. Chen, D. Godovsky, O. Inganäs, J.C. Hummelen, R.A.J. Janssens, M. Svensson, and M.R. Andersson: Polymer photovoltaic devices from stratified multilayers of donor-acceptor blends. *Adv. Mater.* **12,** 1367 (2000).
141. C.J. Brabec, A. Cravino, D. Meissner, N.S. Sariciftci, M.T. Rispens, L. Sanchez, J.C. Hummelen, and T. Fromherz: The influence of materials work function on the open circuit voltage of plastic solar cells. *Thin Solid Films* **403–404,** 368 (2002).
142. M. Drees, K. Premaratne, W. Graupner, J.R. Heflin, R.M. Davis, D. Marciu, and M. Miller: Creation of a gradient polymer-fullerene interface in photovoltaic devices by thermally controlled interdiffusion. *Appl. Phys. Lett.* **81,** 1 (2002).
143. G.G. Malliaras, J.R. Salem, P.J. Brock, and J.C. Scott: Photovoltaic measurement of the built-in potential in organic light emitting diodes and photodiodes. *J. Appl. Phys.* **84,** 1583 (1998).
144. C.J. Brabec, A. Cravino, D. Meissner, N.S. Sariciftci, T. Fromherz, M.T. Rispens, L. Sanchez, and J.C. Hummelen: Origin of the open circuit voltage of plastic solar cells. *Adv. Funct. Mater.* **11,** 374 (2001).
145. V.D. Mihailetchi, P.W.M. Blom, J.C. Hummelen, and M.T. Rispens: Cathode dependence of the open-circuit voltage of polymer:fullerene bulk heterojunction solar cells. *J. Appl. Phys.* **94,** 6849 (2003).
146. I.H. Campbell, S. Rubin, T.A. Zawodzinski, J.D. Kress, R.L. Martin, D.L. Smith, N.N. Barashkov, and J.P. Ferraris: Controlling Schottky energy barriers in organic electronic devices using self-assembled monolayers. *Phys. Rev. B* **54,** 14321 (1996).
147. C.M. Heller, I.H. Campbell, D.L. Smith, N.N. Barashkov, and J.P. Ferraris: Chemical potential pinning due to equilibrium electron transfer at metal/C 60-doped polymer interfaces. *J. Appl. Phys.* **81,** 3227 (1996).
148. Y. Hirose, A. Kahn, V. Aristov, P. Soukiassian, V. Bulovic, and S.R. Forrest: Chemistry and electronic properties of metal-organic semiconductor interfaces: Al, Ti, In, Sn, Ag, and Au on PTCDA. *Phys. Rev. B* **54,** 13748 (1996).
149. H. Ishii, K. Sugiyama, E. Ito, and K. Seki: Energy level alignment and interfacial electronic structures at organic/metal and organic/organic interfaces. *Adv. Mater.* **11,** 605 (1999).
150. L. Yan and Y. Gao: Interfaces in organic semiconductor devices. *Thin Solid Films* **417,** 101 (2002).
151. N. Koch, A. Kahn, J. Ghijsen, J-J. Pireaux, J. Schwartz, R.L. Johnson, and A. Elschner: Conjugated organic molecules on metal versus polymer electrodes: Demonstration of a key energy level alignment mechanism. *Appl. Phys. Lett.* **82,** 70 (2003).
152. D. Cahen and A. Kahn: Electron energetics at surfaces and interfaces: Concepts and experiments. *Adv. Mater.* **15,** 271 (2003).

153. S.C. Veenstra and H.T. Jonkman: Energy-level alignment at metal-organic and organic-organic interfaces. *J. Polym. Sci Polym. Phys.* **41,** 2549 (2003).
154. S.C. Veenstra, A. Heeres, G. Hadziioannou, G.A. Sawatzky, and H.T. Jonkman: On interface dipole layers between C60 and Ag or Au. *Appl. Phys. A* **75,** 661 (2002).
155. C. Melzer, V.V. Krasnikov, and G. Hadziioannou: Organic donor/acceptor photovoltaics: The role of C60/metal interfaces. *Appl. Phys. Lett.* **82,** 3101 (2003).
156. C.C. Wu, C.I. Wu, J.C. Sturm, and A. Kahn: Surface modification of indium tin oxide by plasma treatment: An effective method to improve the efficiency, brightness, and reliability of organic light-emitting devices. *Appl. Phys. Lett.* **70,** 1348 (1997).
157. K. Sugiyama, H. Ishii, Y. Ouchi, and K. Seki: Dependence of indium–tin–oxide work function on surface cleaning method as studied by ultraviolet and x-ray photoemission spectroscopies. *J. Appl. Phys.* **87,** 295 (2000).
158. J.C. Scott, S.A. Carter, S. Karg, and M. Angelopoulos: Polymeric anodes for organic light-emitting diodes. *Synth. Met.* **85,** 1197 (1997).
159. Y. Cao, G. Yu, C. Zhang, R. Menon, and A.J. Heeger: Polymer light-emitting diodes with polyethylene dioxythiophene–polystyrene sulfonate as the transparent anode. *Synth. Met.* **87,** 171 (1997).
160. T.M. Brown, J.S. Kim, R.H. Friend, F. Cacialli, R. Daik, and W.J. Feast: Built-in field electroabsorption spectroscopy of polymer light-emitting diodes incorporating a doped poly(3,4-ethylene dioxythiophene) hole-injection layer. *Appl. Phys. Lett.* **75,** 1679 (1999).
161. C. Ganzorig and M. Fujihira: Chemical modification of indium-tin-oxide electrodes by surface molecular design in *Organic Optoelectronic Materials, Processing and Devices,* edited by S.C. Moss. (Mater. Res. Soc. Symp. Proc. **708,** Warrendale, PA, 2002), p. 83.
162. L.S. Hung, C.W. Tang, and M.G. Mason: Enhanced electron injection in organic electroluminescence devices using an Al/LiF electrode. *Appl. Phys. Lett.* **70,** 152 (1997).
163. G.E. Jabbour, Y. Kawabe, S.E. Shaheen, J.F. Wang, M.M. Morrell, B. Kippelen, and N. Peyghambarian: Highly efficient and bright organic electroluminescent devices with an aluminum cathode. *Appl. Phys. Lett.* **71,** 1762 (1997).
164. C.J. Brabec, S.E. Shaheen, C. Winder, N.S. Sariciftci, and P. Denk: Effect of LiF/metal electrodes on the performance of plastic solar cells. *Appl. Phys. Lett.* **80,** 1288 (2002).
165. F.L. Zhang, M. Johansson, M.R. Anderson, J.C. Hummelen, and O. Inganäs: Polymer solar cells based on MEH-PPV and PCBM. *Synth. Met.* **137,** 1401 (2003).
166. J.K.J. van Duren, J. Loos, F. Morrissey, C.M. Leewis, K.P.H. Kivits, L.J. van IJzendoorn, M.T. Rispens, J.C. Hummelen, and R.A.J. Janssen: In-situ compositional and structural analysis of plastic solar cells. *Adv. Funct. Mater.* **12,** 665 (2002).
167. C.W.T. Bulle-Lieuwma, W.J.H. van Gennip, J.K.J. van Duren, P. Jonkheijm, R.A.J. Janssen, and J.W. Niemantsverdriet: Characterization of polymer solar cells by TOF-SIMS depth profiling. *Appl. Surf. Sci.* **203,** 547 (2003).
168. H. Kim, S-H. Jin, H. Suh, and K. Lee: Origin of the open circuit voltage in conjugated polymer-fullerene photovoltaic cells. In *Organic Photovoltaics IV,* edited by Z.H. Kafafi, and P.A. Lane, Proceedings of the SPIE, Vol. 5215, (SPIE, Bellingham, WA, 2004), p. 111,
169. J. Gao, F. Hide, and H. Wang: Efficient photodetectors and photovoltaic cells from composites of fullerenes and conjugated polymers: Photoinduced electron transfer. *Synth. Met.* **84,** 979 (1997).
170. J. Liu, Y. Shi, and Y. Yang: Solvation-induced morphology effects on the performance of polymer-based photovoltaic devices. *Adv. Funct. Mater.* **11,** 420 (2001).
171. M.C. Scharber, N.A. Schulz, N.S. Sariciftci, and C.J. Brabec: Optical- and photocurrent-detected magnetic resonance studies on conjugated polymer/fullerene composites. *Phys. Rev. B* **67,** 085202 (2003).
172. H. Hoppe, M. Niggemann, C. Winder, J. Kraut, R. Hiesgen, A. Hinsch, D. Meissner, and N.S. Sariciftci: Nanoscale morphology of conjugated polymer/fullerene based bulk-heterojunction solar cells. *Adv. Funct. Mater.* (2004).
173. H. Frohne, S.E. Shaheen, C.J. Brabec, D.C. Müller, N.S. Sariciftci, and K. Meerholz: Influence of the anodic work function on the performance of organic solar cells. *Chem Phys Chem.* **9,** 795 (2002).
174. C.M. Ramsdale, J.A. Barker, A.C. Arias, J.D. MacKenzie, R.H. Friend, and N.C. Greenham: The origin of the open circuit voltage in polyfluorene-based photovoltaic devices. *J. Appl. Phys.* **92,** 4266 (2002).
175. J.A. Barker, C.M. Ramsdale, and N.C. Greenham: Modeling the current-voltage characteristics of bilayer polymer photovoltaic devices. *Phys. Rev. B* **67,** 075205 (2003).
176. I. Riedel, J. Parisi, V. Dyakonov, L. Lutsen, D. Vanderzande, and J.C. Hummelen: Effect of temperature and illumination on the electrical characteristics of polymer-fullerene bulk-heterojunction solar cells. *Adv. Funct. Mater.* **14,** 38 (2004).
177. P. Schilinsky, C. Waldauf, J. Hauch, and C.J. Brabec: Simulation of light intensity dependent current characteristics of polymer solar cells. *J. Appl. Phys.* **95,** 2816 (2004).
178. H. Hoppe, N. Arnold, D. Meissner, and N.S. Sariciftci: Modelling the optical absorption within conjugated polymer/fullerene-based bulk-heterojunction organic solar cells. *Sol. Energy Mater. Sol. Cells* **80,** 105 (2003).
179. J. Drechsel, B. Maennig, D. Gebeyehu, M. Pfeiffer, K. Leo, and H. Hoppe: MIP-type organic solar cells incorporating phthalocyanine/fullerene mixed layers and doped wide-gap transport layers. *Org. Electron.* **5,** 175 (2004).
180. H. Hoppe, N. Arnold, D. Meissner, and N.S. Sariciftci: Modeling of optical absorption in conjugated polymer/fullerene bulk-heterojunction plastic solar cells. *Thin Solid Films* **451,** 589 (2004).
181. I. Riedel and V. Dyakonov: Influence of electronic transport properties of polymer-fullerene blends on the performance of bulk heterojunction photovoltaic devices. *Phys. Status Solidi A* **201,** 1332 (2004).
182. S.E. Shaheen, G.E. Jabbour, M.M. Morrell, Y. Kawabe, B. Kippelen, N. Peyghambarian, M-F. Nabor, R. Schlaf, E.A. Mash, and N.R. Armstrong: Bright blue organic light-emitting diode with improved color purity using a LiF/Al cathode. *J. Appl. Phys.* **84,** 2324 (1998).
183. T.M. Brown, R.H. Friend, I.S. Millard, D.J. Lacey, J.H. Burroughes, and F. Cacialli: LiF/Al cathodes and the effect of LiF thickness on the device characteristics and built-in potential of polymer light-emitting diodes. *Appl. Phys. Lett.* **77,** 3096 (2000).
184. T. Kugler, W.R. Salaneck, H. Rost, and A.B. Holmes: Polymer band alignment at the interface with indium tin oxide: Consequences for light emitting devices. *Chem. Phys. Lett.* **310,** 391 (1999).
185. G. Greczynski, T. Kugler, and W.R. Salaneck: Energy level alignment in organic-based three-layer structures studied by photoelectron spectroscopy. *J. Appl. Phys.* **88,** 7187 (2000).
186. J.Y. Kim, J.H. Jung, D.E. Lee, and J. Joo: Enhancement of electrical conductivity of poly(3,4-ethylenedioxythiophene)/poly(4-styrenesulfonate) by a change of solvents. *Synth. Met.* **126,** 311 (2002).
187. S.K.M. Jönssona, J. Birgerson, X. Crispin, G. Greczynski, W. Osikowicz, A.W.D. van der Gonc, W.R. Salaneck, and M. Fahlman: The effects of solvents on the morphology and sheet resistance in poly(3,4-ethylenedioxythiophene)–polystyrenesulfonic acid (PEDOT–PSS) films. *Synth. Met.* **139,** 1 (2003).

https://doi.org/10.1557/JMR.2004.0252

188. K. Kuhnke, R. Becker, M. Epple, and K. Kern: C60 exciton quenching near metal surfaces. *Phys. Rev. Lett.* **79,** 3246 (1997).
189. P. Würfel: Thermodynamic limitations to solar energy conversion. *Physica E* **14,** 18 (2002).
190. A. Yakimov and S.R. Forrest: High photovoltage multiple-heterojunction organic solar cells incorporating interfacial metallic nanoclusters. *Appl. Phys. Lett.* **80,** 1667 (2002).
191. L.S. Roman, O. Inganäs, T. Granlund, T. Nyberg, M. Svensson, M.R. Andersson, and J.C. Hummelen: Trapping light in polymer photodiodes with soft embossed gratings. *Adv. Mater.* **12,** 189 (2000).
192. M. Niggemann, B. Bläsi, A. Gombert, A. Hinsch, H. Hoppe, P. Lalanne, D. Meissner, and V. Wittwer: Trapping light in organic plastic solar cells with integrated diffraction gratings, presented at the 17th European Photovoltaic Solar Energy Conference, Munich, Germany, 2001.
193. A. Dhanabalan, J.K.J. van Duren, P.A. van Hal, J.L.J. van Dongen, and R.A.J. Janssen: Synthesis and characterization of a low bandgap conjugated polymer for bulk heterojunction photovoltaic cells. *Adv. Funct. Mater.* **11,** 255 (2001).
194. J.K.J. van Duren, A. Dhanabalan, P.A. van Hal, and R.A.J. Janssen: Low-bandgap polymer photovoltaic cells. *Synth. Met.* **121,** 1587 (2001).
195. C.J. Brabec, C. Winder, N.S. Sariciftci, J.C. Hummelen, A. Dhanabalan, P.A. van Hal, and R.A.J. Janssen: A low-bandgap semiconducting polymer for photovoltaic devices and infrared emitting diodes. *Adv. Funct. Mater.* **12,** 709 (2002).
196. K. Colladet, M. Nicolas, L. Goris, L. Lutsen, and D. Vanderzande: Low-band gap polymers for photovoltaic applications. *Thin Solid Films* **451–452,** 7 (2004).
197. N. Camaioni, M. Catellani, S. Luzzati, and A. Migliori: Morphological characterization of poly(3-octylthiophene):plasticizer:C60 blends. *Thin Solid Films* **403–404,** 489 (2002).
198. M.T. Rispens, A. Meetsma, R. Rittberger, C.J. Brabec, N.S. Sariciftci, and J.C. Hummelen: Influence of the solvent on the crystal structure of PCBM and the efficiency of MDMO-PPV:PCBM 'plastic' solar cells. *Chem. Commun.* **17,** 2116 (2003).
199. J.J.M. Halls, A.C. Arias, J.D. MacKenzie, W. Wu, M. Inbasekaran, E.P. Woo, and R.H. Friend: Photodiodes based on polyfluorene composites: Influence of morphology. *Adv. Mater.* **12,** 498 (2000).
200. T. Martens, Z. Beelen, J. D'Haen, T. Munters, L. Goris, J. Manca, M. D'Olieslaeger, D. Vanderzande, L.D. Schepper, and R. Andriessen: Morphology of MDMO-PPV:PCBM bulk heterojunction organic solar cells studied by AFM, KFM and TEM. In *Organic Photovoltaics III,* edited by Z.H. Kafafi and D. Fichou, Proceedings of SPIE Vol. 4801 (SPIE, Bellingham, WA, 2003), p. 40.
201. A.C. Arias, N. Corcoran, M. Banach, R.H. Friend, J.D. MacKenzie, and W.T.S. Huck: Vertically segregated polymer-blend photovoltaic thin-film structures through surface-mediated solution processing. *Appl. Phys. Lett.* **80,** 1695 (2002).
202. N. Camaioni, G. Ridolfi, G. Casalbore-Miceli, G. Possamai, and M. Maggini: The effect of a mild thermal treatment on the performance of poly(3-alkylthiophene)/fullerene solar cells. *Adv. Mater.* **14,** 1735 (2002).
203. M. Hiramoto, K. Suemori, and M. Yokoyama: Photovoltaic properties of ultramicrostructure controlled organic co-deposited films. *Jpn. J. Appl. Phys.* **41,** 2763 (2002).
204. T. Martens, J. D'Haen, T. Munters, Z. Beelen, L. Goris, J. Manca, M. D'Olieslaeger, D. Vanderzande, L.D. Schepper, and R. Andriessen: Disclosure of the nanostructure of MDMO-PPV:PCBM bulk heterojunction organic solar cells by a combination of SPM and TEM. *Synth. Met.* **138,** 243 (2003).
205. H.J. Snaith, A.C. Arias, A.C. Morteani, C. Silva, and R.H. Friend: Charge generation kinetics and transport mechanisms in blended polyfluorene photovoltaic devices. *Nano Lett.* **2,** 1353 (2003).
206. J-F. Eckert, J-F. Nicoud, J-F. Nierengarten, S-G. Liu, L. Echegoyen, F. Barigelletti, N. Armaroli, L. Ouali, V. Krasnikov, and G. Hadziioannou: Fullerene-oligophenylenevinylene hybrids: Synthesis, electronic properties, and incorporation in photovoltaic devices. *J. Am. Chem. Soc.* **122,** 7467 (2000).
207. A. Dhanabalan, J. Knol, J.C. Hummelen, and R.A.J. Janssen: Design and synthesis of new processible donor-acceptor dyad and triads. *Synth. Met.* **119,** 519 (2001).
208. T. Otsubo, Y. Aso, and K. Takimiya: Functional oligothiophenes as advanced molecular electronic materials. *J. Mater. Chem.* **12,** 2565 (2002).
209. G. Possamai, N. Camaioni, G. Ridolfi, L. Franco, M. Ruzzi, E. Menna, G. Casalbore-Miceli, A.M. Fichera, G. Scorrano, C. Corvaja, and M. Maggini: A fullerene-azothiophene dyad for photovoltaics. *Synth. Met.* **139,** 585 (2003).
210. M.A. Loi, P. Denk, H. Hoppe, H. Neugebauer, C. Winder, D. Meissner, C. Brabec, N.S. Sariciftci, A. Gouloumis, P. Vazquez, and T. Torres: Long-lived photoinduced charge separation for solar cell applications in phthalocyanine-fulleropyrrolidine dyad thin films. *J. Mater. Chem.* **13,** 700 (2003).
211. F. Zhang, M. Svensson, M.R. Andersson, M. Maggini, S. Bucella, E. Menna, and O. Inganäs: Soluble polythiophenes with pendant fullerene groups as double cable materials for photodiodes. *Adv. Mater.* **13,** 1871 (2001).
212. A. Cravino, G. Zerza, M. Maggini, S. Bucella, M. Svensson, M.R. Andersson, H. Neugebauer, C.J. Brabec, and N.S. Sariciftci: A soluble donor-acceptor double-cable polymer: Polythiophene with pendant fullerenes. *Monatsh. Chem.* **134,** 519 (2003).
213. C. Park, J. Yoon, and E.L. Thomas: Enabling nanotechnology with self assembled block copolymer patterns. *Polymer* **44,** 6725 (2003).
214. U. Stalmach, B. de Boer, C. Videlot, P.F. van Hutten, and G. Hadziioannou: Semiconducting diblock copolymers synthesized by means of controlled radical polymerization techniques. *J. Am. Chem. Soc.* **122,** 5464 (2000).
215. G. Hadziioannou: Semiconducting block copolymers for self-assembled photovoltaic devices. *MRS Bull.* **27,** 456 (2002).
216. S.S. Sun, Z. Fan, Y. Wang, C. Taft, J. Haliburton, and S. Maaref: Synthesis and characterization of a novel -D-B-A-B- block copolymer system for potential light harvesting applications. In *Organic Photovoltaics III,* edited by Z.H. Kafafi and D. Fichou, Proceedings of SPIE Vol. 4801 (SPIE, Bellingham, WA, 2003), p. 114.
217. T. Kietzke, D. Neher, K. Landfester, R. Montenegro, R. Güntner, and U. Scherf: Novel approaches to polymer blends based on polymer nanoparticles. *Nature Mater.* **2,** 408 (2003).
218. K.M. Coakley, Y. Liu, M.D. McGehee, K. Frindell, and G.D. Stucky: Infiltrating semiconducting polymers into self-assembled mesoporous titania films for photovoltaic applications. *Adv. Funct. Mater.* **13,** 301 (2003).
219. K.M. Coakley and M.D. McGehee: Photovoltaic cells made from conjugated polymers infiltrated into mesoporous titania. *Appl. Phys. Lett.* **83,** 1 (2003).
220. X. Peng, L. Manna, W. Yang, J. Wickham, E. Scher, A. Kadavanich, and A.P. Alivisatos: Shape control of CdSe nanocrystals. *Nature* **404,** 59 (2000).
221. D.J. Milliron, C. Pitois, C. Edder, J.M.J. Frechet, and A.P. Alivisatos: Designed for charge transfer: complexes of CdSe nanocrystals and oligothiophenes, in *Organic and Polymeric Materials and Devices—Optical, Electrical, and Optoelectric Properties,* edited by G.E. Jabbour, S.A. Carter, J. Kido, S-T. Lee, and N.S. Sariciftci. (*Mater. Res. Soc. Symp. Proc.* **725,** Warrendale, PA, 2002), p. 177.